

---

# TEA-Time: Transporting Effects Across Time

---

**Harsh Parikh\***  
Amazon SCOT, Seattle, USA  
Yale University, New Haven, USA

**Gabriel Levin-Konigsberg**  
Amazon SCOT, Seattle, USA

**Dominique Perrault-Joncas**  
Amazon SCOT, Seattle, USA

**Alexander Volfovsky†**  
Amazon SCOT, Seattle, USA  
Duke University, Durham, USA

## Abstract

Treatment effects estimated from randomized controlled trials are local not only to the study population but also to the time at which the trial was conducted. We develop a framework for *temporal transportation*: extrapolating treatment effects to time periods where no experiment was conducted. We target the transported average treatment effect (TATE) and show that under a separable temporal effects assumption, the TATE decomposes into an observed average treatment effect and a temporal ratio. We provide two identification strategies—one using replicated trials comparing the same treatments at different times, another using common treatment arms observed across time—and develop doubly robust, semiparametrically efficient estimators for each. Monte Carlo simulations confirm that both estimators achieve nominal coverage, with the common arm strategy yielding substantial efficiency gains when its stronger assumptions hold. We apply our methods to A/B tests from the Upworthy Research Archive, demonstrating that the two strategies exhibit a variance-bias tradeoff: the common arm approach offers greater precision but may incur bias when treatments interact heterogeneously with temporal factors.

## 1 Introduction

Causal effects identified by randomized controlled trials (RCTs) are inherently local—not only to the population studied but also to the time at which the trial was conducted. A marketing intervention tested during summer may perform differently in holiday season; a job training program evaluated during economic expansion may have different effects during recession; a drug’s efficacy may vary with seasonal disease prevalence. Despite the ubiquity of such temporal variation, the causal inference literature has devoted considerably more attention to transporting effects across populations than across time.

This paper develops a framework for *temporal transportation*: using data from trials conducted at one time to estimate treatment effects at different times. We consider settings where an organization has access to multiple historical RCTs—potentially comparing different interventions—and seeks to predict what the effect of a specific treatment would be if administered at a new target time. This problem arises naturally in e-commerce (where promotional effects exhibit strong seasonality), digital advertising (where effectiveness varies with attention cycles), labor market policy (where program effects depend on market tightness), and clinical trials (where drug efficacy may vary with seasonal disease prevalence).

---

\*Corresponding author: [harsh.parikh@yale.edu](mailto:harsh.parikh@yale.edu)

†Corresponding author: [alexander.volfovsky@duke.edu](mailto:alexander.volfovsky@duke.edu)

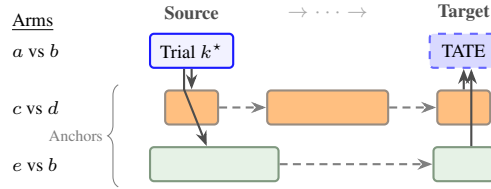


Figure 1: *Temporal transportation uses anchor trials to extrapolate treatment effects across time.* Information flows from the primary trial  $k^*$  (blue) to contemporary anchor trials (orange, green) at the source time, then across time via anchors observed at multiple periods (dashed arrows), and finally from target-time anchors to the transported effect (TATE, dashed blue). This chain identifies how effects scale temporally without requiring the primary comparison at the target time.

The challenge of temporal transportation differs fundamentally from cross-population generalization. When transporting across populations, we typically observe covariates in both source and target and can reweight to adjust for distributional shifts [Dahabreh et al., 2019, Stuart et al., 2011]. When transporting across time, we cannot observe outcomes under the target timing—by definition, we are extrapolating to a period where the relevant trial was not conducted. Identification therefore requires structural assumptions about how treatment effects vary with time.

Our key insight is that *other* trials — comparing potentially different treatments — can serve as temporal anchors. Figure 1 illustrates the core idea. Suppose we observe a primary trial comparing treatments  $a$  versus  $b$  at a source time, and wish to estimate what this effect would be at a target time. If anchor trials testing other treatment comparisons were conducted at both source and target times, we can use them to learn how outcomes or effects evolve temporally.

**Contributions.** Our paper makes three contributions:

First, we formalize the temporal transportation problem and introduce the *transported average treatment effect* (TATE) as the target estimand. Under a *separable temporal effects* assumption—a multiplicative decomposition of potential outcomes into unit-specific and time-specific components—we show that the TATE equals the product of an observed average treatment effect and an identifiable temporal ratio.

Second, we provide two identification strategies with distinct data requirements. The *replicated trials* strategy uses pairs of trials comparing identical treatments at different times, permitting flexible temporal structures but requiring exact replication. The *common arm* strategy identifies the temporal ratio from any treatment arm observed at multiple times—such as a control arm appearing across many trials—but imposes a stronger restriction that temporal effects operate only through measurement time.

Third, we develop doubly robust estimators for the TATE under each strategy. Our estimators are consistent if either the outcome model or the propensity scores are correctly specified, and achieve the semiparametric efficiency bound when both are correct. For the common arm strategy with multiple anchors, we derive the optimally weighted combination.

We evaluate our methods through simulations and an application to over 22,000 A/B tests from the Upworthy Research Archive [Matias et al., 2021]. The simulations confirm near-nominal coverage, with the common arm strategy achieving approximately 50% lower RMSE when its assumptions hold. The empirical application reveals a variance-bias tradeoff: the common arm approach offers greater precision but incurs bias when the temporal factor depends on both intervention and measurement times.

## 2 Setup and Assumptions

**Notation.** Let  $\mathcal{T}$  denote discrete time periods,  $\mathcal{P}$  a population of units, and  $\mathcal{A} \cup \{0\}$  the set of treatments with 0 as control. We observe a collection of RCTs  $\mathcal{K}$ . Each trial  $k \in \mathcal{K}$  draws a sample  $S_k \subset \mathcal{P}$  of  $n_k$  units, compares treatment  $a_k$  against baseline  $b_k$ , administers treatment at time  $t_{0k}$ , and measures outcomes at time  $t_{1k} \geq t_{0k}$ . Units in trial  $k$  are randomly assigned to  $A \in \{a_k, b_k\}$ . Let  $X$  denote pre-treatment covariates and  $S \in \mathcal{K}$  denote trial membership.

Define  $Y_{t_1}(a, t_0)$  as the potential outcome under treatment  $a$  administered at  $t_0$  and measured at  $t_1$ . The observed outcome for a unit in trial  $k$  is  $Y_{t_{1k}} = Y_{t_{1k}}(A, t_{0k})$ .

**Standard assumptions.** We maintain standard experimental assumptions: (i) *random assignment*:  $A \perp \{Y_{t_1}(a, t_0)\}_{a, t_0, t_1} \mid S = k$  for each trial  $k$ ; and (ii) *SUTVA*: no interference between units and no hidden treatment versions.

**Separable temporal effects.** To enable temporal transportation, we impose multiplicative structure on how outcomes vary with timing.

**Assumption 1** (Separable Temporal Effects). *Potential outcomes satisfy  $Y_{t_1}(a, t_0) = \theta_a(X) \cdot \Lambda(t_0, t_1) + \epsilon_{t_1}$ , where  $\theta_a(X)$  is a unit-specific response function,  $\Lambda(t_0, t_1)$  is a temporal modifier common across units and treatments, and  $\mathbb{E}[\epsilon_{t_1} \mid X, A] = 0$ .*

This structure is analogous to a rank-one factor model:  $\theta_a(X)$  serves as unit-specific loadings and  $\Lambda(t_0, t_1)$  as the time factor. Under Assumption 1, the individual treatment effect  $Y_{t_1}(a, t_0) - Y_{t_1}(b, t_0) = \tilde{\theta}_{a,b}(X) \cdot \Lambda(t_0, t_1)$ , where  $\tilde{\theta}_{a,b}(X) := \theta_a(X) - \theta_b(X)$ .

**Target estimand.** The *transported average treatment effect* (TATE) for trial  $k^*$  is  $\tau(a_{k^*}, b_{k^*}, t_{0k^*}, t_{1k^*}, \delta_0, \delta_1) = \tau_{k^*}(\delta_0, \delta_1) =$

$$\mathbb{E}[[Y_{t_{1k^*} + \delta_1}(a_{k^*}, t_{0k^*} + \delta_0) - Y_{t_{1k^*} + \delta_1}(b_{k^*}, t_{0k^*} + \delta_0)] \mid S = k^*], \quad (1)$$

representing the ATE for the trial  $k^*$  population had treatment occurred at time  $t_{0k^*} + \delta_0$  with outcomes measured at  $t_{1k^*} + \delta_1$ .

### 3 Identification

We establish identification of the TATE in two steps: first decomposing it into an observed ATE and a temporal ratio, then providing two strategies for identifying the ratio from auxiliary trials.

#### 3.1 TATE Decomposition

Our first result shows that under separable temporal effects, the TATE factors into two components: the treatment effect observed in the original trial and a ratio capturing how temporal conditions scale outcomes.

**Theorem 1** (TATE Decomposition). *Under random assignment, SUTVA, and Assumption 1:*

$$\tau_{k^*}(\delta_0, \delta_1) = \tau_{k^*}(0, 0) \cdot \frac{\Lambda(t_{0k^*} + \delta_0, t_{1k^*} + \delta_1)}{\Lambda(t_{0k^*}, t_{1k^*})}, \quad (2)$$

where  $\tau_{k^*}(0, 0) = \mathbb{E}[Y_{t_{1k^*}} \mid A = a_{k^*}, S = k^*] - \mathbb{E}[Y_{t_{1k^*}} \mid A = b_{k^*}, S = k^*]$  is the observed ATE.

The intuition is straightforward. Under separability, both the observed and transported treatment effects share the same unit-specific component  $\tilde{\theta}_{a_{k^*}, b_{k^*}, k^*} := \mathbb{E}[\tilde{\theta}_{a_{k^*}, b_{k^*}}(X) \mid S = k^*]$ , differing only in their temporal multipliers. Taking ratios cancels this common factor, leaving only the ratio of temporal modifiers.

Theorem 1 reduces TATE identification to identifying the temporal ratio  $\Lambda(t_{0k^*} + \delta_0, t_{1k^*} + \delta_1) / \Lambda(t_{0k^*}, t_{1k^*})$ . We now present two strategies for achieving this, each with distinct data requirements and structural assumptions.

#### 3.2 Strategy 1: Replicated Trials

The first strategy identifies temporal ratios using trials that compare the same treatment pair at different times. The key insight is that if two trials test identical treatments but at different times, the ratio of their ATEs reveals how temporal conditions scale effects.

For treatments  $a, b \in \mathcal{A} \cup \{0\}$  with  $a > b$ , define  $\mathcal{K}(a, b) := \{\ell \in \mathcal{K} : (a_\ell, b_\ell) = (a, b)\}$  as the set of trials comparing  $a$  against  $b$ , and  $\mathcal{T}(a, b) := \{(t_{0\ell}, t_{1\ell}) : \ell \in \mathcal{K}(a, b)\}$  as the timing pairs at which this comparison was conducted.

**Assumption 2** (Replicated Trials). (i) Each trial draws an independent random sample from  $\mathcal{P}$ , with  $Y(a) \perp S \mid X$ . (ii) There exists an anchor pair  $(a^*, b^*)$  with  $\bar{\theta}_{a^*, b^*} := \mathbb{E}[\bar{\theta}_{a^*, b^*}(X)] \neq 0$  and  $\Lambda(t_0, t_1) \neq 0$  for all  $(t_0, t_1) \in \mathcal{T}(a^*, b^*)$ . (iii) Both source and target timing belong to  $\mathcal{T}(a^*, b^*)$ .

The random sampling condition ensures that trial-specific effects reflect population quantities. The anchor pair conditions guarantee that ATE ratios are well-defined and informative. The temporal coverage condition requires that the anchor comparison was conducted at both the original and target times.

**Theorem 2** (Identification via Replicated Trials). *Under Assumption 2, for trials  $\ell, \ell' \in \mathcal{K}(a^*, b^*)$  conducted at times  $(t_{0\ell}, t_{1\ell}) = (t_0, t_1)$  and  $(t_{0\ell'}, t_{1\ell'}) = (t'_0, t'_1)$ :*

$$\frac{\Lambda(t_0, t_1)}{\Lambda(t'_0, t'_1)} = \frac{\tau_\ell(0, 0)}{\tau_{\ell'}(0, 0)}. \quad (3)$$

Under random sampling, both trials draw from the same population, so their average unit-specific effects are identical. Taking ratios of observed ATEs cancels this common factor, yielding the temporal ratio. Notably, the anchor pair  $(a^*, b^*)$  need not equal the target comparison  $(a_{k^*}, b_{k^*})$ —any replicated comparison spanning the relevant times can serve as an anchor.

### 3.3 Strategy 2: Common Arm

The second strategy identifies temporal ratios from a single treatment arm observed at multiple times. This approach is often more practical, as it does not require exact replication of treatment comparisons, but it imposes a stronger structural restriction.

**Assumption 3** (Measurement-Time Structure). *The temporal modifier depends only on measurement time:  $\Lambda(t_0, t_1) = \Lambda(t_1)$  for all  $t_0 \leq t_1$ .*

This assumption is plausible when temporal variation reflects conditions at outcome measurement—such as seasonal demand patterns, economic conditions, or user engagement cycles—rather than conditions at treatment administration.

For treatment  $c \in \mathcal{A} \cup \{0\}$ , define  $\mathcal{K}[c] := \{\ell \in \mathcal{K} : c \in \{a_\ell, b_\ell\}\}$  as trials where  $c$  appears as either arm, and  $\mathcal{T}^{(c)} := \{t_{1\ell} : \ell \in \mathcal{K}[c]\}$  as the measurement times at which  $c$  was observed.

**Assumption 4** (Common Arm). (i) Each trial draws an independent random sample from  $\mathcal{P}$ . (ii) There exists an anchor arm  $c^* \in \mathcal{A} \cup \{0\}$  with  $\bar{\theta}_{c^*} := \mathbb{E}[\theta_{c^*}(X)] \neq 0$ . (iii)  $\{t_{1k^*}, t_{1k^*} + \delta_1\} \subseteq \mathcal{T}^{(c^*)}$ .

Note that Assumption 4(ii) requires non-zero mean outcome under  $c^*$ , rather than a non-zero treatment effect as in Strategy 1. This condition is typically weaker when outcomes are naturally positive.

**Theorem 3** (Identification via Common Arm). *Under Assumptions 1, 3, and 4, for trials  $\ell, \ell' \in \mathcal{K}[c^*]$  with  $t_{1\ell} = t_{1k^*} + \delta_1$  and  $t_{1\ell'} = t_{1k^*}$ :*

$$\frac{\Lambda(t_{1k^*} + \delta_1)}{\Lambda(t_{1k^*})} = \frac{\mathbb{E}[Y_{t_{1\ell}} \mid A = c^*, S = \ell]}{\mathbb{E}[Y_{t_{1\ell'}} \mid A = c^*, S = \ell']}. \quad (4)$$

Under Assumption 3, the expected outcome for units receiving  $c^*$  is  $\mathbb{E}[Y_{t_1} \mid A = c^*] = \bar{\theta}_{c^*} \cdot \Lambda(t_1)$ . Since  $\bar{\theta}_{c^*}$  is constant across trials by random sampling, the ratio of conditional means at different times equals the temporal ratio. The anchor arm  $c^*$  can be any treatment—not necessarily control—providing flexibility when certain treatments appear more frequently across trials.

### 3.4 Comparing the Two Strategies

The two strategies impose different structural requirements. Strategy 1 permits  $\Lambda(t_0, t_1)$  to depend on both treatment administration and measurement times, accommodating settings where intervention timing matters—for instance, if treatment effects decay with elapsed time since administration. However, Strategy 1 requires trials comparing the exact same treatment pair at different times, which may be demanding in practice.

Strategy 2 requires only that some treatment arm appears at multiple measurement times, a condition often satisfied by control arms or standard treatments appearing across many trials. The cost is

the restriction  $\Lambda(t_0, t_1) = \Lambda(t_1)$ , which rules out dependence on intervention timing. When both strategies are feasible, comparing their estimates provides a robustness check; discrepancies suggest potential violations of Assumption 3.

## 4 Estimation and Inference

We develop estimators for the TATE based on the identification results of Section 3. Our approach proceeds in three steps: we derive efficient influence functions from the identified functionals, construct doubly robust estimators, and characterize their asymptotic properties.

### 4.1 Efficient Influence Functions

We observe i.i.d. data  $\{(Y_i, A_i, S_i, X_i)\}_{i=1}^n$ . Define the nuisance functions  $\pi_k(X) := P(S = k | X)$ ,  $e_k(a, X) := P(A = a | S = k, X)$ ,  $\mu_{a,k}(X) := \mathbb{E}[Y | A = a, S = k, X]$ .

Our identification results express the TATE as products and ratios of conditional means. We derive influence functions for these building blocks, then apply the delta method to obtain influence functions for the TATE.

**Building blocks.** The marginal mean  $\bar{\mu}_{a,k} := \mathbb{E}[Y | A = a, S = k]$  has efficient influence function  $\phi_{\bar{\mu}_{a,k}}(O) =$

$$\frac{\mathbf{1}[S = k]}{\pi_k(X)} \left\{ \frac{\mathbf{1}[A = a]}{e_k(a, X)} (Y - \mu_{a,k}(X)) + \mu_{a,k}(X) \right\} - \bar{\mu}_{a,k}.$$

The ATE for trial  $k$ ,  $\tau_k := \tau_k(0, 0) = \bar{\mu}_{a_k, k} - \bar{\mu}_{b_k, k}$ , has influence function  $\phi_{\tau_k}(O) = \phi_{\bar{\mu}_{a_k, k}}(O) - \phi_{\bar{\mu}_{b_k, k}}(O)$ .

**TATE influence functions.** Applying the delta method to the identified functionals yields influence functions for each strategy. For Strategy 1, the TATE is  $\psi_1 = g(\tau_{k^*}, \tau_j, \tau_{j'})$  where  $g(x, y, z) = xy/z$ . The gradient  $\nabla g(x, y, z) = (y/z, x/z, -xy/z^2)^\top$  evaluated at the true parameters gives:

**Proposition 1** (Efficient Influence Functions). *The efficient influence functions for the TATE under each strategy are:*

$$\phi_{\psi_1}(O) = R_1 \cdot \phi_{\tau_{k^*}}(O) + \frac{\psi_1}{\tau_j} \phi_{\tau_j}(O) - \frac{\psi_1}{\tau_{j'}} \phi_{\tau_{j'}}(O), \quad (5)$$

$$\phi_{\psi_2}(O) = R_2 \cdot \phi_{\tau_{k^*}}(O) + \frac{\psi_2}{\bar{\mu}_{c^*, \ell}} \phi_{\bar{\mu}_{c^*, \ell}}(O) - \frac{\psi_2}{\bar{\mu}_{c^*, \ell'}} \phi_{\bar{\mu}_{c^*, \ell'}}(O), \quad (6)$$

where  $R_1 = \tau_j/\tau_{j'}$  and  $R_2 = \bar{\mu}_{c^*, \ell}/\bar{\mu}_{c^*, \ell'}$  are the temporal ratios.

Both influence functions decompose into three terms reflecting distinct sources of uncertainty: the target trial ATE (first term) and both components of the temporal ratio (second and third terms). The coefficients have natural interpretations:  $R_1$  (or  $R_2$ ) scales the target trial's contribution since  $\psi = \tau_{k^*} \cdot R$ , while the terms  $\psi_1/\tau_j$  and  $\psi_1/\tau_{j'}$  reflect how ratio estimation error propagates through the product.

These influence functions satisfy Neyman orthogonality with respect to the nuisance functions. Let  $\eta = (\pi_k, e_k, \mu_{a,k})$  denote the nuisance vector, then the pathwise derivative of  $\mathbb{E}[\phi_{\bar{\mu}_{a,k}}(O; \eta)]$  with respect to  $\eta$  vanishes at the true parameter values  $\left. \frac{\partial}{\partial r} \mathbb{E}[\phi_{\bar{\mu}_{a,k}}(O; \eta + r(\tilde{\eta} - \eta)) \right]_{r=0} = 0$  for all directions  $\tilde{\eta} - \eta$  in the tangent space. This orthogonality implies that first-order errors in nuisance estimation do not affect the estimator's first-order bias, enabling valid inference even when nuisances are estimated at slower-than-parametric rates.

### 4.2 Doubly Robust Estimators

The TATE is a smooth function of identified quantities —  $\psi_1 = g(\tau_{k^*}, \tau_j, \tau_{j'})$  where  $g(x, y, z) = xy/z$  — so we estimate it by plugging in efficient estimates of the building blocks. Define the

doubly robust score  $\varphi_{a,k}(O; \eta) =$

$$\frac{\mathbf{1}[S = k]}{\pi_k(X)} \left\{ \frac{\mathbf{1}[A = a]}{e_k(a, X)} (Y - \mu_{a,k}(X)) + \mu_{a,k}(X) \right\}, \quad (7)$$

where  $\eta = \{\pi_k, e_k, \mu_{a,k}\}$ . This score satisfies  $\mathbb{E}[\varphi_{a,k}(O; \eta)] = \bar{\mu}_{a,k}$ , with centered version  $\phi_{\bar{\mu}_{a,k}}(O) = \varphi_{a,k}(O; \eta) - \bar{\mu}_{a,k}$  being the EIF. Let  $\varphi_{\tau_k}(O; \eta) = \varphi_{a_k,k}(O; \eta) - \varphi_{b_k,k}(O; \eta)$ .

Given estimated nuisances  $\hat{\eta}$ , the building blocks  $\hat{\mu}_{a,k} = \mathbb{P}_n[\varphi_{a,k}(O; \hat{\eta})]$  and  $\hat{\tau}_k = \mathbb{P}_n[\varphi_{\tau_k}(O; \hat{\eta})]$  are asymptotically linear with the EIFs under Assumption 6. The TATE estimators follow by plug-in:

$$\hat{\psi}_1 = \hat{\tau}_{k^*} \cdot \frac{\hat{\tau}_j}{\hat{\tau}_{j'}} \quad (\text{Strategy 1}), \quad (8)$$

$$\hat{\psi}_2 = \hat{\tau}_{k^*} \cdot \frac{\hat{\mu}_{c^*,\ell}}{\hat{\mu}_{c^*,\ell'}} \quad (\text{Strategy 2}). \quad (9)$$

A Taylor expansion combined with asymptotic linearity of the building blocks yields  $\hat{\psi}_1 - \psi_1 = \mathbb{P}_n[\phi_{\psi_1}(O)] + o_p(n^{-1/2})$ , establishing that the plug-in estimator achieves the semiparametric efficiency bound (Appendix B.3). Alternative constructions such as TMLE are asymptotically equivalent (Appendix B.6).

### 4.3 Variance Characterization

The influence functions characterize asymptotic variances via  $V = \mathbb{E}[\phi_{\psi}(O)^2]$ . When the target trial is distinct from anchor trials, the influence function components have disjoint support, yielding:

$$V_{\psi_1} = R_1^2 \cdot V_{\tau_{k^*}} + \psi_1^2 \left( \frac{V_{\tau_j}}{\tau_j^2} + \frac{V_{\tau_{j'}}}{\tau_{j'}^2} \right), \quad (10)$$

$$V_{\psi_2} = R_2^2 \cdot V_{\tau_{k^*}} + \psi_2^2 \left( \frac{V_{\bar{\mu}_{c^*,\ell}}}{\bar{\mu}_{c^*,\ell}^2} + \frac{V_{\bar{\mu}_{c^*,\ell'}}}{\bar{\mu}_{c^*,\ell'}^2} \right). \quad (11)$$

The first term in each expression represents uncertainty from estimating the target trial's ATE, scaled by the squared temporal ratio. The second term captures uncertainty from estimating the temporal ratio itself, scaled by the squared TATE. When  $|R_1|$  or  $|R_2|$  is large (substantial temporal scaling), target trial uncertainty dominates; when the TATE is large, ratio uncertainty becomes more consequential.

**Efficiency comparison.** These expressions reveal why Strategy 2 typically achieves greater precision. The key difference lies in the second term: Strategy 1 involves  $V_{\tau_j}/\tau_j^2$  and  $V_{\tau_{j'}}/\tau_{j'}^2$ , while Strategy 2 involves  $V_{\bar{\mu}_{c^*,\ell}}/\bar{\mu}_{c^*,\ell}^2$  and  $V_{\bar{\mu}_{c^*,\ell'}}/\bar{\mu}_{c^*,\ell'}^2$ .

For Strategy 1, the variance of a treatment effect satisfies:

$$V_{\tau_k} = V_{\bar{\mu}_{a_k,k}} + V_{\bar{\mu}_{b_k,k}} - 2\text{Cov}(\phi_{\bar{\mu}_{a_k,k}}, \phi_{\bar{\mu}_{b_k,k}}). \quad (12)$$

Under randomization, units receive either treatment or control but not both, so the covariance term is typically small. Thus  $V_{\tau_k} \approx V_{\bar{\mu}_{a_k,k}} + V_{\bar{\mu}_{b_k,k}}$ , meaning Strategy 1's ratio involves roughly twice the variance of Strategy 2's.

Moreover, treatment effects are typically smaller in magnitude than outcome means:  $|\tau_k| \ll |\bar{\mu}_{a,k}|$  in many applications. This implies  $V_{\tau_k}/\tau_k^2 \gg V_{\bar{\mu}_{a,k}}/\bar{\mu}_{a,k}^2$ —the coefficient of variation for treatment effects exceeds that for means. Both factors compound to give Strategy 2 substantially lower variance for the temporal ratio, which propagates to the final TATE estimator. This efficiency gain comes at the cost of Assumption 3; when this assumption fails, Strategy 2 incurs bias while Strategy 1 remains valid.

#### 4.4 Multiple Anchor Arms

When  $m \geq 2$  anchor arms satisfy Assumption 4, each yields a ratio  $R_{2,j} = \bar{\mu}_{c_j, \ell_j} / \bar{\mu}_{c_j, \ell'_j}$  identifying the same temporal quantity. Let  $\hat{\mathbf{R}} = (\hat{R}_{2,1}, \dots, \hat{R}_{2,m})^\top$  with influence functions:

$$\phi_{R_{2,j}}(O) = \frac{1}{\bar{\mu}_{c_j, \ell'_j}} \phi_{\bar{\mu}_{c_j, \ell_j}}(O) - \frac{R_{2,j}}{\bar{\mu}_{c_j, \ell'_j}} \phi_{\bar{\mu}_{c_j, \ell'_j}}(O). \quad (13)$$

The covariance matrix  $\mathbf{V}_{\mathbf{R}} = \mathbb{E}[\phi_{\mathbf{R}}(O)\phi_{\mathbf{R}}(O)^\top]$  captures both the variance of individual ratios and their correlations (which arise when anchors share trials at common time points).

**Optimal combination.** Among estimators of the form  $\hat{R} = \mathbf{w}^\top \hat{\mathbf{R}}$  with  $\mathbf{w}^\top \mathbf{1} = 1$ , the minimum-variance choice is:

$$\mathbf{w}^* = \frac{\mathbf{V}_{\mathbf{R}}^{-1} \mathbf{1}}{\mathbf{1}^\top \mathbf{V}_{\mathbf{R}}^{-1} \mathbf{1}}, \quad V_{R^*} = \frac{1}{\mathbf{1}^\top \mathbf{V}_{\mathbf{R}}^{-1} \mathbf{1}}. \quad (14)$$

This yields  $\hat{R}_2^* = \mathbf{w}^{*\top} \hat{\mathbf{R}}$  and  $\hat{\psi}_2^* = \hat{\tau}_{k^*} \cdot \hat{R}_2^*$ . The optimal variance  $V_{R^*}$  is no larger than any individual  $V_{R_{2,j}}$ , with strict improvement when anchors provide non-redundant information. In practice,  $\mathbf{V}_{\mathbf{R}}$  is replaced by its sample analog  $\hat{\mathbf{V}}_{\mathbf{R}} = \mathbb{P}_n[\hat{\phi}_{\mathbf{R}}(O)\hat{\phi}_{\mathbf{R}}(O)^\top]$ .

#### 4.5 Asymptotic Properties

We establish formal guarantees under regularity conditions.

**Assumption 5** (Regularity). (i) Overlap:  $\pi_k(X) > \epsilon$  and  $e_k(a, X) > \epsilon$  a.s. for some  $\epsilon > 0$ . (ii) Bounded moments:  $\mathbb{E}[Y^4] < \infty$ . (iii) Non-degeneracy:  $\tau_{j'} \neq 0$  (Strategy 1) or  $\bar{\mu}_{c^*, \ell'} \neq 0$  (Strategy 2).

The overlap condition ensures inverse probability weights remain bounded. Bounded fourth moments guarantee finite variance of the influence function. Non-degeneracy ensures the temporal ratio is well-defined; division by zero would invalidate the identification strategy.

**Assumption 6** (Nuisance Estimation Rates).  $\|\hat{\mu}_{a,k} - \mu_{a,k}\|_2 \cdot (\|\hat{\pi}_k - \pi_k\|_2 + \|\hat{e}_k - e_k\|_2) = o_p(n^{-1/2})$ .<sup>3</sup>

**Theorem 4** (Asymptotic Properties). *Under Assumptions 5–6 and the relevant identification assumptions:*

- (a) Asymptotic normality:  $\sqrt{n}(\hat{\psi} - \psi) \xrightarrow{d} \mathcal{N}(0, V)$  for  $\hat{\psi} \in \{\hat{\psi}_1, \hat{\psi}_2, \hat{\psi}_2^*\}$ , where  $V = \mathbb{E}[\phi_\psi(O)^2]$  is the semiparametric efficiency bound.
- (b) Double robustness: Estimators are consistent if, for each  $(k, a)$ , either  $\mu_{a,k}(X)$  or both  $\pi_k(X)$  and  $e_k(a, X)$  are correctly specified.<sup>4</sup>
- (c) Efficiency: When all models are correct, estimators achieve the semiparametric efficiency bound. The combined estimator  $\hat{\psi}_2^*$  achieves minimum variance among linear combinations of anchor-specific ratios.

**Variance estimation and inference.** The asymptotic variance is consistently estimated by:

$$\hat{V} = \mathbb{P}_n[\hat{\phi}_\psi(O)^2], \quad (15)$$

where  $\hat{\phi}_\psi(O)$  substitutes estimated nuisances and parameters into the influence function. This yields asymptotically valid confidence intervals  $\hat{\psi} \pm z_{1-\alpha/2} \sqrt{\hat{V}/n}$  and Wald tests of hypotheses about the TATE.

<sup>3</sup>This product rate condition is weaker than requiring  $n^{-1/2}$  convergence of individual nuisances. It is satisfied when each nuisance converges at  $n^{-1/4}$  rate, achievable by many machine learning methods with appropriate regularization.

<sup>4</sup>In randomized trials, treatment propensities  $e_k(a, X)$  are known by design, providing one layer of robustness automatically. This makes the outcome model specification less critical for consistency, though correct specification still improves efficiency.

When using flexible machine learning methods for nuisance estimation,  $K$ -fold cross-fitting ensures Assumption 6 holds under weak conditions: partition data into  $K$  folds, estimate nuisances on  $K - 1$  folds, and evaluate scores on the held-out fold. This sample-splitting avoids overfitting bias without sacrificing efficiency asymptotically.

## 5 Related Work

Having established our framework, we now position it relative to existing literature. Our contribution sits at the intersection of several research streams, but differs from each in important ways.

**Transportability and external validity.** The literature on generalizing experimental findings to new populations [Huang and Parikh, 2024, Degtiar and Rose, 2023, Bareinboim and Pearl, 2016, Cole and Stuart, 2010, Westreich et al., 2017] typically assumes access to covariate information in the target population and leverages selection-on-observables and positivity assumptions. Our setting differs in that the “target” is defined by *temporal shift* rather than *covariate shift*.

**Meta-analysis.** Meta-analytic methods [Borenstein et al., 2021, Higgins et al., 2009, Riley et al., 2011, Parikh et al., 2025] synthesize evidence across studies and can incorporate time as a study-level moderator. However, the goal is typically *pooling*—estimating an average effect or characterizing heterogeneity across observed studies—rather than *extrapolation* to counterfactual timing.

**Factor models, synthetic control, and difference-in-differences.** Our separable temporal effects assumption (Assumption 1) shares structural similarities with several literatures that leverage factor structure for causal inference. Interactive fixed effects models in panel econometrics [Bai, 2009] decompose outcomes into unit-specific loadings and time-specific factors; matrix completion approaches [Athey et al., 2021] view the potential outcome matrix as approximately low-rank; and synthetic control [Abadie et al., 2010, 2015] and difference-in-differences methods [Callaway and Sant’Anna, 2021, Sun and Abraham, 2021, Goodman-Bacon, 2021, De Chaisemartin and D’Haultfœuille, 2020, Borusyak et al., 2024] implicitly rely on factor structure to construct counterfactuals, a connection made explicit by Xu [2017] and Arkhangelsky et al. [2021].

Our separability assumption (A.1) is similar to this broader literature. However, our setting and goals differ in three key respects. *First*, these methods estimate effects or impute missing outcomes *within* the observed temporal support of the study; we *extrapolate* to timing configurations where the relevant trial was not conducted. *Second*, our setup involves integrating information from multiple trials comparing different intervention or treatment pairs. *Third*, existing methods use outcomes from control units to impute missing potential outcome for the treated unit; we instead use outcomes from trials with *entirely different treatments* to identify how effects scale across time.

**Semiparametric estimation.** Our estimation approach builds on the semiparametric efficiency literature [Robins et al., 1994, Bang and Robins, 2005, Kennedy, 2022, Parikh et al., 2025], particularly doubly robust methods and debiased machine learning [Chernozhukov et al., 2018].

## 6 Simulation Study

We conduct Monte Carlo simulations to evaluate finite-sample performance, assessing bias, variance, and coverage while comparing the two identification strategies.

### 6.1 Design

**Data generating process.** We generate data according to Assumption 1. Units have covariates  $X = (X_1, X_2)^\top$  with  $X_1 \sim \mathcal{N}(0, 1)$  and  $X_2 \sim \text{Bernoulli}(0.5)$ . The temporal modifier captures seasonal variation through  $\Lambda(t) = 1 + \gamma \sin(2\pi t/12)$  with  $\gamma = 0.3$ , producing a 12-period cycle. For treatment  $a \in \{0, 1, 2\}$ , potential outcomes follow

$$Y_{t_1}(a, t_0) = \theta_a(X) \cdot \Lambda(t_1) + \epsilon, \quad \epsilon \sim \mathcal{N}(0, 1),$$

where  $\theta_0(X) = 2 + 0.5X_1 + 0.3X_2$ ,  $\theta_1(X) = \theta_0(X) + 1 + 0.4X_1 + 0.2X_2$ , and  $\theta_2(X) = \theta_0(X) + 0.5 + 0.2X_1 + 0.1X_2$ .

Table 1: Trial configurations ( $n_k = n/6$ , treatment probability 0.5).

$k$	$(a_k, b_k)$	$(t_{0k}, t_{1k})$	Role
1	(1, 0)	(1, 3)	Target trial
2	(1, 0)	(7, 9)	Strategy 1 anchor (target time)
3	(1, 0)	(1, 3)	Strategy 1 anchor (source time)
4	(2, 0)	(1, 3)	Strategy 2 anchor (source time)
5	(2, 0)	(7, 9)	Strategy 2 anchor (target time)
6	(1, 0)	(4, 6)	Additional trial

Table 2: Simulation results ( $\gamma = 0.3$ ).

$n$	Estimator	Bias	RMSE	SE Ratio	Coverage
600	Oracle	-.010	.136	1.10	.952
	S1	+.026	.341	1.01	.940
	S2-C	-.007	.180	1.10	.944
	S2-T	-.004	.159	1.28	.964
	S2-M	-.013	.158	1.09	.950
1200	Oracle	+.002	.087	1.17	.972
	S1	+.010	.205	1.12	.962
	S2-C	+.008	.130	1.05	.952
	S2-T	+.003	.106	1.33	.984
	S2-M	+.000	.105	1.13	.962
2400	Oracle	+.003	.061	1.15	.980
	S1	+.004	.143	1.08	.966
	S2-C	+.007	.085	1.09	.972
	S2-T	+.003	.070	1.38	.992
	S2-M	+.003	.071	1.13	.980

**Trial structure.** We simulate  $K = 6$  trials as detailed in Table 1. The target trial  $k^* = 1$  compares treatment 1 against control at  $(t_{0k^*}, t_{1k^*}) = (1, 3)$ , and we estimate the TATE at  $(t_0, t_1) = (7, 9)$ —a half-cycle displacement with true value  $\psi \approx 0.77$ . Trials 2–3 provide anchors for Strategy 1; trials 4–5 provide anchor arms for Strategy 2.

**Estimators.** We compare five estimators: S1 implements Strategy 1 using trials 2 and 3; S2-C and S2-T implement Strategy 2 with control ( $c^* = 0$ ) and treatment 2 ( $c^* = 2$ ) as anchors, respectively; S2-M combines both anchors via inverse-variance weighting; and Oracle uses the true temporal ratio, providing a lower bound on achievable variance. Nuisance functions are estimated via gradient boosting with 5-fold cross-fitting. We vary  $n \in \{600, 1200, 2400\}$  with  $B = 500$  replications.

## 6.2 Results

Table 2 presents bias, RMSE, the ratio of estimated to empirical standard errors (SE Ratio), and coverage of 95% confidence intervals.

**Bias and consistency.** All estimators exhibit negligible bias across sample sizes (absolute bias  $< 0.03$  even at  $n = 600$ ), confirming that identification assumptions hold and doubly robust estimators achieve the consistency guaranteed by Theorem 4.

**Efficiency comparison.** Strategy 2 substantially outperforms Strategy 1 in RMSE. At  $n = 2400$ , S2-M achieves RMSE of 0.071 versus 0.143 for S1—a 50% reduction. This gain arises because Strategy 2 estimates temporal ratios from conditional means rather than treatment contrasts, which have higher variance. The multi-anchor estimator S2-M performs comparably to single-anchor variants.

**Variance estimation and coverage.** SE Ratios near 1.0 confirm accurate variance estimation. S2-T shows mildly elevated ratios (1.28–1.38), reflecting finite-sample variability with a single anchor.

Table 3: Estimation performance relative to true TATE

	Trial A		Trial B	
	S1	S2	S1	S2
RMSE	.0062	.0080	.0090	.0101
Bias	−.0002	+.0067	+.0012	−.0046
Avg Std Err	.0054	.0019	.0053	.0018
Correlation	.71	.35	.52	.18

Coverage rates are at or above nominal 95% for all estimators, with slight overcoverage for S2-T consistent with conservative variance estimation.

**Comparison to oracle.** The Oracle provides a lower bound on achievable RMSE by eliminating uncertainty in the temporal ratio. At  $n = 2400$ , S2-M achieves RMSE of 0.071 versus 0.061 for Oracle, indicating that estimation error stems primarily from the target trial ATE rather than temporal ratio estimation.

**Summary.** The simulations validate our theoretical results: both strategies yield consistent estimators with accurate variance estimation and near-nominal coverage. When Assumption 3 holds, Strategy 2 reduces RMSE by approximately 50% compared to Strategy 1, and combining multiple anchors provides modest additional gains.

## 7 Empirical Application: Upworthy Headline Tests

We apply our framework to headline A/B tests from the Upworthy Research Archive [Matias et al., 2021], one of the largest publicly available collections of randomized digital experiments. Full details appear in Appendix C.

**Data and setup.** Upworthy conducted over 22,000 headline A/B tests between 2013–2015, randomly assigning visitors to different headline-image combinations and measuring click-through rates (CTR). Following Matias et al. [2021], we exclude tests from June 2013–January 2014 where randomization problems were detected.

To apply our framework, we must identify treatment arms appearing across multiple tests at different times. Since each test uses unique headline text, we cluster semantically similar headlines using Sentence-BERT embeddings [Reimers and Gurevych, 2019] with a constrained clustering procedure ensuring no two headlines from the same test share a cluster (see Appendix C.2). This yields 50 headline clusters, each appearing across multiple months.

**Research question.** We estimate TATEs for two A/B tests conducted in late 2013 and early 2014, transporting observed effects to subsequent months of 2014. We compare both identification strategies against a “ground truth” TATE constructed by pooling all available comparisons of the same cluster pair at each target time.

**Results.** Figure 2 and Table 3 reveal a variance-bias tradeoff. Strategy 2 yields substantially smaller standard errors than Strategy 1 (mean SE of 0.0019 vs. 0.0054 for Trial A), reflecting its use of conditional means rather than treatment contrasts. However, Strategy 2 exhibits systematic bias: estimates remain nearly constant across months while the true TATE varies considerably—even changing sign in some months. Strategy 1, despite wider confidence bands, tracks these dynamics (correlation with true TATE: 0.71 vs. 0.35 for Trial A). This pattern suggests violations of Assumption 3: the temporal factor depends not only on measurement time but also on intervention time. This occurs when the gap between intervention and measurement matters—for instance, if treatment effects decay over time. Strategy 1 accommodates such dependence by allowing  $\Lambda(t_0, t_1)$  to vary with both arguments.

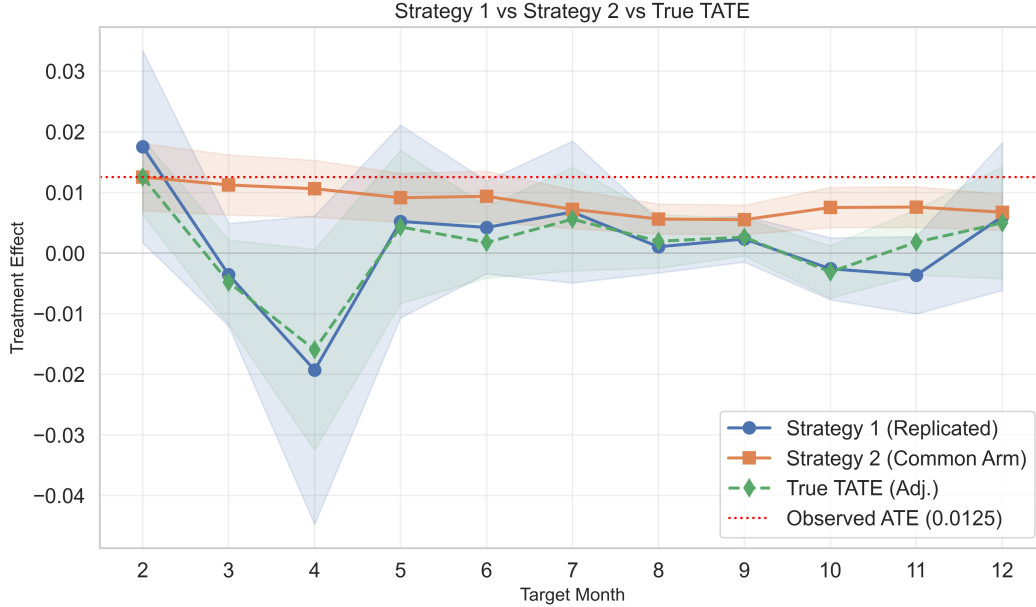


Figure 2: TATE estimates for Trial A (Cluster 17 vs. 10) by target month. Strategy 1 (blue) exhibits higher variance but tracks the true TATE (green); Strategy 2 (orange) is more precise but shows systematic bias. Shaded regions indicate 95% CIs.

## 8 Discussion and Conclusion

We have developed a framework for transporting treatment effects across time, introducing the transported average treatment effect (TATE) and providing identification and estimation strategies under a separable temporal effects assumption. We conclude by discussing key considerations and limitations.

**The separability assumption.** Our identification relies on potential outcomes decomposing multiplicatively into unit-specific and temporal components (Assumption 1). This structure is plausible when temporal variation operates as a scaling factor affecting all units proportionally—for instance, seasonal demand shocks in retail, attention cycles in digital advertising, or labor market tightness for employment interventions. The assumption may fail when ceiling/floor effects attenuate temporal scaling for some units, or when treatments exhibit qualitative interactions with time (helping some subgroups in certain periods while hurting them in others). When multiple anchor arms are available, there are testable implications providing a diagnostic.

**Strategy selection.** The replicated trials strategy (Strategy 1) permits flexible temporal structures where  $\Lambda(t_0, t_1)$  depends on both treatment and measurement times, but requires trials comparing identical treatment pairs across time—a demanding data requirement. The common arm strategy (Strategy 2) requires only that some treatment arm appears at multiple measurement times, offering greater practical flexibility since control arms often span many trials. The cost is the stronger restriction  $\Lambda(t_0, t_1) = \Lambda(t_1)$ , appropriate when temporal effects reflect conditions at outcome measurement rather than treatment administration. When both strategies are feasible, comparing estimates provides a robustness check.

**Limitations.** The separability assumption is fundamentally untestable from data at observed times alone. Furthermore, our approach relies on population stability across time; if population compositions drift over time, temporal effects are conflated with compositional changes. We also assume treatment stability—that the “same” treatment does not differ in implementation across time.

**Future Work.** Two promising extensions address key limitations of our framework. *Sensitivity Analysis for Separability Violations:* Our identification relies critically on Assumption 1, which

is fundamentally untestable. A natural extension develops sensitivity analysis tools quantifying how departures from multiplicative separability propagate to bias in the TATE. This would transform our point identification results into partial identification intervals, providing more robust uncertainty quantification when separability is violated. *Covariate-Dependent Temporal Modifiers*: Our temporal modifier  $\Lambda(t_0, t_1)$  is assumed common across units, ruling out heterogeneous temporal effects across subpopulations. Future work would accommodate covariate-dependent modifiers  $\Lambda(t_0, t_1; X)$ .

**Conclusion.** This paper makes three contributions. First, we formalized temporal transportation through the TATE and showed it decomposes into an observed ATE and a temporal ratio under separability. Second, we provided two identification strategies with different data requirements and structural restrictions, offering practitioners flexibility based on available trials. Third, we developed doubly robust estimators achieving semiparametric efficiency, with valid inference through influence function-based variance estimation. Temporal variation in treatment effects is ubiquitous yet understudied relative to population heterogeneity. As organizations increasingly rely on continuous experimentation, transporting findings across time becomes essential: a promotion tested in January must inform March decisions; a program evaluated during expansion must guide policy during contraction. Our framework provides principled tools for such extrapolation, grounded in explicit assumptions that can be deliberated in context.

## References

- Alberto Abadie, Alexis Diamond, and Jens Hainmueller. Synthetic control methods for comparative case studies: Estimating the effect of California’s tobacco control program. *Journal of the American Statistical Association*, 105(490):493–505, 2010.
- Alberto Abadie, Alexis Diamond, and Jens Hainmueller. Comparative politics and the synthetic control method. *American Journal of Political Science*, 59(2):495–510, 2015.
- Dmitry Arkhangelsky, Susan Athey, David A Hirshberg, Guido W Imbens, and Stefan Wager. Synthetic difference-in-differences. *American Economic Review*, 111(12):4088–4118, 2021.
- Susan Athey, Mohsen Bayati, Nikolay Doudchenko, Guido Imbens, and Khashayar Khosravi. Matrix completion methods for causal panel data models. *Journal of the American Statistical Association*, 116(536):1716–1730, 2021.
- Jushan Bai. Panel data models with interactive fixed effects. *Econometrica*, 77(4):1229–1279, 2009.
- Heejung Bang and James M Robins. Doubly robust estimation in missing data and causal inference models. *Biometrics*, 61(4):962–973, 2005.
- Elias Bareinboim and Judea Pearl. Causal inference and the data-fusion problem. *Proceedings of the National Academy of Sciences*, 113(27):7345–7352, 2016.
- Michael Borenstein, Larry V Hedges, Julian PT Higgins, and Hannah R Rothstein. *Introduction to Meta-Analysis*. Wiley, Chichester, 2nd edition, 2021.
- Kirill Borusyak, Xavier Jaravel, and Jann Spiess. Revisiting event study designs: Robust and efficient estimation. *Review of Economic Studies*, 91(6):3253–3285, 2024.
- Brantly Callaway and Pedro HC Sant’Anna. Difference-in-differences with multiple time periods. *Journal of Econometrics*, 225(2):200–230, 2021.
- Victor Chernozhukov, Denis Chetverikov, Mert Demirer, Esther Duflo, Christian Hansen, Whitney Newey, and James Robins. Double/debiased machine learning for treatment and structural parameters. *The Econometrics Journal*, 21(1):C1–C68, 2018.
- Stephen R Cole and Elizabeth A Stuart. Generalizing evidence from randomized clinical trials to target populations: The actg 320 trial. *American Journal of Epidemiology*, 172(1):107–115, 2010.
- Issa J Dahabreh, Sarah E Robertson, Eric J Tchetgen Tchetgen, Elizabeth A Stuart, and Miguel A Hernán. Generalizing causal inferences from individuals in randomized trials to all trial-eligible individuals. *Biometrics*, 75(2):685–694, 2019.

- Clément De Chaisemartin and Xavier D’Haultfoeuille. Two-way fixed effects estimators with heterogeneous treatment effects. *American Economic Review*, 110(9):2964–2996, 2020.
- Irina Degtiar and Sherri Rose. A review of generalizability and transportability. *Annual Review of Statistics and Its Application*, 10(1):501–524, 2023.
- Andrew Goodman-Bacon. Difference-in-differences with variation in treatment timing. *Journal of Econometrics*, 225(2):254–277, 2021.
- Julian PT Higgins, Simon G Thompson, and David J Spiegelhalter. A re-evaluation of random-effects meta-analysis. *Journal of the Royal Statistical Society: Series A*, 172(1):137–159, 2009.
- Melody Y Huang and Harsh Parikh. Towards generalizing inferences from trials to target populations. *Harvard Data Science Review*, 6(4), 2024.
- Edward H Kennedy. Semiparametric doubly robust targeted double machine learning: A review. *arXiv preprint arXiv:2203.06469*, 2022.
- Harold W Kuhn. The Hungarian method for the assignment problem. *Naval Research Logistics Quarterly*, 2(1-2):83–97, 1955.
- J. Nathan Matias, Kevin Munger, Marianne Aubin Le Quere, and Charles Ebersole. The Upworthy Research Archive: A time series of 32,487 experiments in U.S. media. *Scientific Data*, 8(1):1–6, 2021.
- Harsh Parikh, Marco Morucci, Vittorio Orlandi, Sudeepa Roy, Cynthia Rudin, and Alexander Volfovsky. A double machine learning approach for combining experimental and observational studies. *Observational Studies*, 11(3):249–300, 2025.
- Nils Reimers and Iryna Gurevych. Sentence-BERT: Sentence embeddings using Siamese BERT-networks. In *Proceedings of the 2019 Conference on Empirical Methods in Natural Language Processing and the 9th International Joint Conference on Natural Language Processing (EMNLP-IJCNLP)*, pages 3982–3992. Association for Computational Linguistics, 2019.
- Richard D Riley, Julian PT Higgins, and Jonathan J Deeks. Interpretation of random effects meta-analyses. *BMJ*, 342:d549, 2011.
- James M Robins, Andrea Rotnitzky, and Lue Ping Zhao. Estimation of regression coefficients when some regressors are not always observed. *Journal of the American Statistical Association*, 89(427):846–866, 1994.
- Elizabeth A Stuart, Stephen R Cole, Catherine P Bradshaw, and Philip J Leaf. The use of propensity scores to assess the generalizability of results from randomized trials. *Journal of the Royal Statistical Society: Series A*, 174(2):369–386, 2011.
- Liyang Sun and Sarah Abraham. Estimating dynamic treatment effects in event studies with heterogeneous treatment effects. *Journal of Econometrics*, 225(2):175–199, 2021.
- Aad W van der Vaart. *Asymptotic Statistics*. Cambridge University Press, Cambridge, 1998.
- Daniel Westreich, Jessie K Edwards, Catherine R Lesko, Elizabeth Stuart, and Stephen R Cole. Transportability of trial results using inverse odds of sampling weights. *American Journal of Epidemiology*, 186(8):1010–1014, 2017.
- Yiqing Xu. Generalized synthetic control method: Causal inference with interactive fixed effects models. *Political Analysis*, 25(1):57–76, 2017.

## A Proofs for Identification Results

*Proof of Theorem 1.* Under random assignment and SUTVA, the observed ATE is identified by:

$$\begin{aligned}\tau_{k^*}(0, 0) &= \mathbb{E}[Y_{t_{1k^*}}(a_{k^*}, t_{0k^*}) - Y_{t_{1k^*}}(b_{k^*}, t_{0k^*}) \mid S = k^*] \\ &= \mathbb{E}[Y_{t_{1k^*}} \mid A = a_{k^*}, S = k^*] - \mathbb{E}[Y_{t_{1k^*}} \mid A = b_{k^*}, S = k^*].\end{aligned}$$

Under Assumption 1, we have:

$$\begin{aligned}Y_{t_1}(a, t_0) - Y_{t_1}(b, t_0) &= \theta_a(X) \cdot \Lambda(t_0, t_1) + \epsilon_{t_1} - \theta_b(X) \cdot \Lambda(t_0, t_1) - \epsilon_{t_1} \\ &= \tilde{\theta}_{a,b}(X) \cdot \Lambda(t_0, t_1),\end{aligned}$$

where  $\tilde{\theta}_{a,b}(X) := \theta_a(X) - \theta_b(X)$ . Therefore:

$$\begin{aligned}\tau_{k^*}(0, 0) &= \mathbb{E}[\tilde{\theta}_{a_{k^*}, b_{k^*}}(X) \cdot \Lambda(t_{0k^*}, t_{1k^*}) \mid S = k^*] \\ &= \mathbb{E}[\tilde{\theta}_{a_{k^*}, b_{k^*}}(X) \mid S = k^*] \cdot \Lambda(t_{0k^*}, t_{1k^*}) \\ &= \bar{\tilde{\theta}}_{a_{k^*}, b_{k^*}, k^*} \cdot \Lambda(t_{0k^*}, t_{1k^*}),\end{aligned}$$

where  $\bar{\tilde{\theta}}_{a_{k^*}, b_{k^*}, k^*} := \mathbb{E}[\tilde{\theta}_{a_{k^*}, b_{k^*}}(X) \mid S = k^*]$ .

Similarly, the transported ATE satisfies:

$$\begin{aligned}\tau_{k^*}(\delta_0, \delta_1) &= \mathbb{E}[Y_{t_{1k^*} + \delta_1}(a_{k^*}, t_{0k^*} + \delta_0) - Y_{t_{1k^*} + \delta_1}(b_{k^*}, t_{0k^*} + \delta_0) \mid S = k^*] \\ &= \mathbb{E}[\tilde{\theta}_{a_{k^*}, b_{k^*}}(X) \cdot \Lambda(t_{0k^*} + \delta_0, t_{1k^*} + \delta_1) \mid S = k^*] \\ &= \bar{\tilde{\theta}}_{a_{k^*}, b_{k^*}, k^*} \cdot \Lambda(t_{0k^*} + \delta_0, t_{1k^*} + \delta_1).\end{aligned}$$

Taking the ratio:

$$\frac{\tau_{k^*}(\delta_0, \delta_1)}{\tau_{k^*}(0, 0)} = \frac{\bar{\tilde{\theta}}_{a_{k^*}, b_{k^*}, k^*} \cdot \Lambda(t_{0k^*} + \delta_0, t_{1k^*} + \delta_1)}{\bar{\tilde{\theta}}_{a_{k^*}, b_{k^*}, k^*} \cdot \Lambda(t_{0k^*}, t_{1k^*})} = \frac{\Lambda(t_{0k^*} + \delta_0, t_{1k^*} + \delta_1)}{\Lambda(t_{0k^*}, t_{1k^*})},$$

which yields (2).  $\square$

*Proof of Theorem 2.* Under the random sampling condition in Assumption 2(i), for any trial  $\ell \in \mathcal{K}(a^*, b^*)$ :

$$\bar{\tilde{\theta}}_{a^*, b^*, \ell} := \mathbb{E}[\tilde{\theta}_{a^*, b^*}(X) \mid S = \ell] = \mathbb{E}[\tilde{\theta}_{a^*, b^*}(X)] =: \bar{\tilde{\theta}}_{a^*, b^*},$$

where the second equality follows from  $Y(a) \perp S \mid X$  and random sampling from the common population  $\mathcal{P}$ .

By the same argument as in Theorem 1, for any  $\ell \in \mathcal{K}(a^*, b^*)$ :

$$\tau_\ell(0, 0) = \bar{\tilde{\theta}}_{a^*, b^*} \cdot \Lambda(t_{0\ell}, t_{1\ell}).$$

Thus, for any  $\ell, \ell' \in \mathcal{K}(a^*, b^*)$ :

$$\frac{\tau_\ell(0, 0)}{\tau_{\ell'}(0, 0)} = \frac{\bar{\tilde{\theta}}_{a^*, b^*} \cdot \Lambda(t_{0\ell}, t_{1\ell})}{\bar{\tilde{\theta}}_{a^*, b^*} \cdot \Lambda(t_{0\ell'}, t_{1\ell'})} = \frac{\Lambda(t_{0\ell}, t_{1\ell})}{\Lambda(t_{0\ell'}, t_{1\ell'})}.$$

Division is valid because  $\bar{\tilde{\theta}}_{a^*, b^*} \neq 0$  by Assumption 2(ii) and  $\Lambda(t_{0\ell'}, t_{1\ell'}) \neq 0$  by the same assumption. Setting  $(t_{0\ell}, t_{1\ell}) = (t_0, t_1)$  and  $(t_{0\ell'}, t_{1\ell'}) = (t'_0, t'_1)$  yields (3).  $\square$

*Proof of Theorem 3.* Under Assumption 1 with treatment  $c^*$ :

$$Y_{t_1}(c^*, t_0) = \theta_{c^*}(X) \cdot \Lambda(t_0, t_1) + \epsilon_{t_1}.$$

Under Assumption 3,  $\Lambda(t_0, t_1) = \Lambda(t_1)$ , so:

$$Y_{t_1}(c^*, t_0) = \theta_{c^*}(X) \cdot \Lambda(t_1) + \epsilon_{t_1}.$$

For units receiving treatment  $c^*$  in trial  $\ell \in \mathcal{K}[c^*]$ , by random assignment:

$$\begin{aligned}\mathbb{E}[Y_{t_{1\ell}} \mid A = c^*, S = \ell] &= \mathbb{E}[Y_{t_{1\ell}}(c^*, t_{0\ell}) \mid S = \ell] \\ &= \mathbb{E}[\theta_{c^*}(X) \cdot \Lambda(t_{1\ell}) + \epsilon_{t_{1\ell}} \mid S = \ell] \\ &= \mathbb{E}[\theta_{c^*}(X) \mid S = \ell] \cdot \Lambda(t_{1\ell}),\end{aligned}$$

where the last equality uses  $\mathbb{E}[\epsilon_{t_{1\ell}} \mid X, A] = 0$ .

Under the random sampling condition in Assumption 4(i):

$$\mathbb{E}[\theta_{c^*}(X) \mid S = \ell] = \mathbb{E}[\theta_{c^*}(X)] = \bar{\theta}_{c^*}$$

for all  $\ell \in \mathcal{K}[c^*]$ .

Therefore, for any  $\ell, \ell' \in \mathcal{K}[c^*]$ :

$$\frac{\mathbb{E}[Y_{t_{1\ell}} \mid A = c^*, S = \ell]}{\mathbb{E}[Y_{t_{1\ell'}} \mid A = c^*, S = \ell']} = \frac{\bar{\theta}_{c^*} \cdot \Lambda(t_{1\ell})}{\bar{\theta}_{c^*} \cdot \Lambda(t_{1\ell'})} = \frac{\Lambda(t_{1\ell})}{\Lambda(t_{1\ell'})}.$$

Division is valid because  $\bar{\theta}_{c^*} \neq 0$  by Assumption 4(ii) and  $\Lambda(t_{1\ell'}) \neq 0$  by Assumption 5(iii).

Setting  $t_{1\ell} = t_{1k^*} + \delta_1$  and  $t_{1\ell'} = t_{1k^*}$ , and applying Assumption 3 to express the left-hand side of (2):

$$\frac{\Lambda(t_{0k^*} + \delta_0, t_{1k^*} + \delta_1)}{\Lambda(t_{0k^*}, t_{1k^*})} = \frac{\Lambda(t_{1k^*} + \delta_1)}{\Lambda(t_{1k^*})} = \frac{\mathbb{E}[Y_{t_{1\ell}} \mid A = c^*, S = \ell]}{\mathbb{E}[Y_{t_{1\ell'}} \mid A = c^*, S = \ell']},$$

which yields (4). □

## B Proofs for Estimation Results

### B.1 Properties of Doubly Robust Scores

**Lemma 1** (Properties of Doubly Robust Scores). *Under random assignment, SUTVA, and Assumption 5(i)–(ii), the score  $\varphi_{a,k}(O; \eta)$  defined in (7) satisfies:*

- (i) Unbiasedness:  $\mathbb{E}[\varphi_{a,k}(O; \eta)] = \bar{\mu}_{a,k}$ .
- (ii) Neyman orthogonality: *The pathwise derivative with respect to each nuisance function vanishes at the truth.*
- (iii) Bounded variance:  $\mathbb{E}[\varphi_{a,k}(O; \eta)^2] < \infty$ .

Consequently,  $\phi_{\bar{\mu}_{a,k}}(O) = \varphi_{a,k}(O; \eta) - \bar{\mu}_{a,k}$  is the efficient influence function for  $\bar{\mu}_{a,k}$ .

*Proof. Part (i): Unbiasedness.* We compute the expectation of each term in (7). For the first term inside the braces:

$$\begin{aligned}\mathbb{E}\left[\frac{\mathbf{1}[S = k]}{\pi_k(X)} \cdot \frac{\mathbf{1}[A = a]}{e_k(a, X)} (Y - \mu_{a,k}(X))\right] \\ = \mathbb{E}\left[\frac{\mathbf{1}[S = k]}{\pi_k(X)} \cdot \frac{\mathbf{1}[A = a]}{e_k(a, X)} \mathbb{E}[Y - \mu_{a,k}(X) \mid A, S, X]\right] = 0,\end{aligned}$$

since  $\mathbb{E}[Y \mid A = a, S = k, X] = \mu_{a,k}(X)$  by definition.

For the second term:

$$\begin{aligned}\mathbb{E}\left[\frac{\mathbf{1}[S = k]}{\pi_k(X)} \mu_{a,k}(X)\right] &= \mathbb{E}\left[\mathbb{E}\left[\frac{\mathbf{1}[S = k]}{\pi_k(X)} \mid X\right] \mu_{a,k}(X)\right] \\ &= \mathbb{E}\left[\frac{P(S = k \mid X)}{\pi_k(X)} \mu_{a,k}(X)\right] \\ &= \mathbb{E}[\mu_{a,k}(X)] \\ &= \bar{\mu}_{a,k}.\end{aligned}$$

*Part (ii): Neyman orthogonality.* We verify that the pathwise derivative with respect to each nuisance component vanishes at the true parameter values.

*Derivative with respect to  $\mu_{a,k}$ :* Let  $\mu_{a,k}^r = \mu_{a,k} + r(\tilde{\mu}_{a,k} - \mu_{a,k})$  for  $r \in [0, 1]$ . Then:

$$\frac{\partial}{\partial r} \mathbb{E}[\varphi_{a,k}(O; \pi_k, e_k, \mu_{a,k}^r)] \Big|_{r=0} = \mathbb{E} \left[ \frac{\mathbf{1}[S = k]}{\pi_k(X)} \left( 1 - \frac{\mathbf{1}[A = a]}{e_k(a, X)} \right) (\tilde{\mu}_{a,k}(X) - \mu_{a,k}(X)) \right].$$

Conditioning on  $(S, X)$ :

$$\mathbb{E} \left[ 1 - \frac{\mathbf{1}[A = a]}{e_k(a, X)} \mid S = k, X \right] = 1 - \frac{P(A = a \mid S = k, X)}{e_k(a, X)} = 1 - 1 = 0.$$

Hence the derivative vanishes.

*Derivative with respect to  $e_k$ :* Let  $e_k^r(a, X) = e_k(a, X) + r(\tilde{e}_k(a, X) - e_k(a, X))$ . Then:

$$\begin{aligned} \frac{\partial}{\partial r} \mathbb{E}[\varphi_{a,k}(O; \pi_k, e_k^r, \mu_{a,k})] \Big|_{r=0} \\ = \mathbb{E} \left[ \frac{\mathbf{1}[S = k]}{\pi_k(X)} \cdot \frac{-\mathbf{1}[A = a]}{e_k(a, X)^2} (Y - \mu_{a,k}(X)) (\tilde{e}_k(a, X) - e_k(a, X)) \right]. \end{aligned}$$

Conditioning on  $(S, X)$  and using  $\mathbb{E}[Y - \mu_{a,k}(X) \mid A = a, S = k, X] = 0$ :

$$\mathbb{E} \left[ \frac{\mathbf{1}[A = a]}{e_k(a, X)^2} (Y - \mu_{a,k}(X)) \mid S = k, X \right] = \frac{e_k(a, X)}{e_k(a, X)^2} \cdot \mathbb{E}[Y - \mu_{a,k}(X) \mid A = a, S = k, X] = 0.$$

*Derivative with respect to  $\pi_k$ :* Let  $\pi_k^r(X) = \pi_k(X) + r(\tilde{\pi}_k(X) - \pi_k(X))$ . Then:

$$\begin{aligned} \frac{\partial}{\partial r} \mathbb{E}[\varphi_{a,k}(O; \pi_k^r, e_k, \mu_{a,k})] \Big|_{r=0} \\ = \mathbb{E} \left[ \frac{-\mathbf{1}[S = k]}{\pi_k(X)^2} (\tilde{\pi}_k(X) - \pi_k(X)) \left\{ \frac{\mathbf{1}[A = a]}{e_k(a, X)} (Y - \mu_{a,k}(X)) + \mu_{a,k}(X) \right\} \right]. \end{aligned}$$

Conditioning on  $X$ :

$$\begin{aligned} \mathbb{E} \left[ \mathbf{1}[S = k] \left\{ \frac{\mathbf{1}[A = a]}{e_k(a, X)} (Y - \mu_{a,k}(X)) + \mu_{a,k}(X) \right\} \mid X \right] \\ = P(S = k \mid X) \cdot \mathbb{E} \left[ \frac{\mathbf{1}[A = a]}{e_k(a, X)} (Y - \mu_{a,k}(X)) + \mu_{a,k}(X) \mid S = k, X \right] \\ = \pi_k(X) \cdot \mu_{a,k}(X), \end{aligned}$$

where we used the fact that the first term inside the expectation has conditional mean zero (shown in part (i)). Thus:

$$\frac{\partial}{\partial r} \mathbb{E}[\varphi_{a,k}(O; \pi_k^r, e_k, \mu_{a,k})] \Big|_{r=0} = \mathbb{E} \left[ \frac{-(\tilde{\pi}_k(X) - \pi_k(X))}{\pi_k(X)} \mu_{a,k}(X) \right].$$

This equals zero when evaluated at the true  $\pi_k$ , since the derivative is with respect to perturbations around the truth and  $\tilde{\pi}_k - \pi_k$  integrates to zero for valid perturbations in the tangent space.

*Part (iii): Bounded variance.* Assumption 5(i) ensures  $\pi_k(X)^{-1} \leq \epsilon^{-1}$  and  $e_k(a, X)^{-1} \leq \epsilon^{-1}$  almost surely. Combined with Assumption 5(ii) giving  $\mathbb{E}[Y^4] < \infty$ , the Cauchy-Schwarz inequality yields:

$$\mathbb{E}[\varphi_{a,k}(O; \eta)^2] \leq \epsilon^{-4} \mathbb{E} \left[ \left( \frac{\mathbf{1}[A = a]}{e_k(a, X)} |Y - \mu_{a,k}(X)| + |\mu_{a,k}(X)| \right)^2 \right] < \infty.$$

□

## B.2 Derivation of Influence Functions

**Proposition 2** (Influence Function for Strategy 1). *The influence function for  $\psi_1 = \tau_{k^*} \cdot \tau_j / \tau_{j'}$  is given by (5).*

*Proof.* The estimand  $\psi_1 = g(\tau_{k^*}, \tau_j, \tau_{j'})$  where  $g(x, y, z) = x \cdot y / z$ . By the delta method for influence functions:

$$\phi_{\psi_1}(O) = \frac{\partial g}{\partial x} \phi_{\tau_{k^*}}(O) + \frac{\partial g}{\partial y} \phi_{\tau_j}(O) + \frac{\partial g}{\partial z} \phi_{\tau_{j'}}(O).$$

Computing the partial derivatives at  $(\tau_{k^*}, \tau_j, \tau_{j'})$ :

$$\begin{aligned} \frac{\partial g}{\partial x} &= \frac{y}{z} = \frac{\tau_j}{\tau_{j'}} = R_1, \\ \frac{\partial g}{\partial y} &= \frac{x}{z} = \frac{\tau_{k^*}}{\tau_{j'}} = \frac{\tau_{k^*} \cdot \tau_j / \tau_{j'}}{\tau_j} = \frac{\psi_1}{\tau_j}, \\ \frac{\partial g}{\partial z} &= -\frac{xy}{z^2} = -\frac{\tau_{k^*} \tau_j}{\tau_{j'}^2} = -\frac{\psi_1}{\tau_{j'}}. \end{aligned}$$

Substituting yields:

$$\phi_{\psi_1}(O) = R_1 \cdot \phi_{\tau_{k^*}}(O) + \frac{\psi_1}{\tau_j} \phi_{\tau_j}(O) - \frac{\psi_1}{\tau_{j'}} \phi_{\tau_{j'}}(O).$$

□

**Proposition 3** (Influence Function for Strategy 2). *The influence function for  $\psi_2 = \tau_{k^*} \cdot \bar{\mu}_{c^*, \ell} / \bar{\mu}_{c^*, \ell'}$  is given by (6).*

*Proof.* The estimand  $\psi_2 = g(\tau_{k^*}, \bar{\mu}_{c^*, \ell}, \bar{\mu}_{c^*, \ell'})$  where  $g(x, y, z) = x \cdot y / z$ . The same delta method argument as in Proposition 2 yields:

$$\phi_{\psi_2}(O) = R_2 \cdot \phi_{\tau_{k^*}}(O) + \frac{\psi_2}{\bar{\mu}_{c^*, \ell}} \phi_{\bar{\mu}_{c^*, \ell}}(O) - \frac{\psi_2}{\bar{\mu}_{c^*, \ell'}} \phi_{\bar{\mu}_{c^*, \ell'}}(O),$$

where  $R_2 = \bar{\mu}_{c^*, \ell} / \bar{\mu}_{c^*, \ell'}$ .

□

**Proposition 4** (Influence Function for Ratio Components). *The influence function for  $R_{2,j} = \bar{\mu}_{c_j, \ell_j} / \bar{\mu}_{c_j, \ell'_j}$  is:*

$$\phi_{R_{2,j}}(O) = \frac{1}{\bar{\mu}_{c_j, \ell'_j}} \phi_{\bar{\mu}_{c_j, \ell_j}}(O) - \frac{R_{2,j}}{\bar{\mu}_{c_j, \ell'_j}} \phi_{\bar{\mu}_{c_j, \ell'_j}}(O).$$

*Proof.* For  $h(y, z) = y / z$ , the delta method gives:

$$\phi_{R_{2,j}}(O) = \frac{\partial h}{\partial y} \phi_{\bar{\mu}_{c_j, \ell_j}}(O) + \frac{\partial h}{\partial z} \phi_{\bar{\mu}_{c_j, \ell'_j}}(O) = \frac{1}{\bar{\mu}_{c_j, \ell'_j}} \phi_{\bar{\mu}_{c_j, \ell_j}}(O) - \frac{\bar{\mu}_{c_j, \ell_j}}{\bar{\mu}_{c_j, \ell'_j}^2} \phi_{\bar{\mu}_{c_j, \ell'_j}}(O).$$

Using  $R_{2,j} = \bar{\mu}_{c_j, \ell_j} / \bar{\mu}_{c_j, \ell'_j}$  gives the result.

□

**Proposition 5** (Influence Function for Combined Estimator). *The influence function for  $\psi_2^* = \tau_{k^*} \cdot R_2^*$  with  $R_2^* = \sum_{j=1}^m w_j^* R_{2,j}$  is:*

$$\phi_{\psi_2^*}(O) = R_2^* \cdot \phi_{\tau_{k^*}}(O) + \tau_{k^*} \sum_{j=1}^m w_j^* \phi_{R_{2,j}}(O).$$

*Proof.* The estimand  $\psi_2^* = \tau_{k^*} \cdot \sum_{j=1}^m w_j^* R_{2,j}$  is a smooth function of  $(\tau_{k^*}, R_{2,1}, \dots, R_{2,m})$ . By the delta method:

$$\begin{aligned}\phi_{\psi_2^*}(O) &= \frac{\partial \psi_2^*}{\partial \tau_{k^*}} \phi_{\tau_{k^*}}(O) + \sum_{j=1}^m \frac{\partial \psi_2^*}{\partial R_{2,j}} \phi_{R_{2,j}}(O) \\ &= R_2^* \cdot \phi_{\tau_{k^*}}(O) + \sum_{j=1}^m \tau_{k^*} w_j^* \phi_{R_{2,j}}(O) \\ &= R_2^* \cdot \phi_{\tau_{k^*}}(O) + \tau_{k^*} \sum_{j=1}^m w_j^* \phi_{R_{2,j}}(O).\end{aligned}$$

□

### B.3 Deriving Efficient Estimators from the EIF

The TATE is a smooth function of identified quantities:  $\psi_1 = g(\tau_{k^*}, \tau_j, \tau_{j'})$  where  $g(x, y, z) = xy/z$ . We show that plug-in estimation with doubly robust building blocks yields semiparametrically efficient estimators.

The doubly robust score for  $\bar{\mu}_{a,k}$  is:

$$\varphi_{a,k}(O; \eta) = \frac{\mathbf{1}[S = k]}{\pi_k(X)} \left\{ \frac{\mathbf{1}[A = a]}{e_k(a, X)} (Y - \mu_{a,k}(X)) + \mu_{a,k}(X) \right\}. \quad (16)$$

This score satisfies  $\mathbb{E}[\varphi_{a,k}(O; \eta)] = \bar{\mu}_{a,k}$  at the true nuisances, and the centered score  $\phi_{\bar{\mu}_{a,k}}(O) = \varphi_{a,k}(O; \eta) - \bar{\mu}_{a,k}$  is the efficient influence function.

Under Assumption 6, the estimator  $\hat{\bar{\mu}}_{a,k} = \mathbb{P}_n[\varphi_{a,k}(O; \hat{\eta})]$  satisfies:

$$\hat{\bar{\mu}}_{a,k} - \bar{\mu}_{a,k} = \mathbb{P}_n[\phi_{\bar{\mu}_{a,k}}(O)] + o_p(n^{-1/2}). \quad (17)$$

The  $o_p(n^{-1/2})$  remainder arises from Neyman orthogonality: the cross-term involving nuisance estimation error is second-order. Similarly,  $\hat{\tau}_k = \mathbb{P}_n[\varphi_{\tau_k}(O; \hat{\eta})]$  satisfies:

$$\hat{\tau}_k - \tau_k = \mathbb{P}_n[\phi_{\tau_k}(O)] + o_p(n^{-1/2}). \quad (18)$$

Consider the plug-in estimator  $\hat{\psi}_1 = g(\hat{\tau}_{k^*}, \hat{\tau}_j, \hat{\tau}_{j'}) = \hat{\tau}_{k^*} \cdot \hat{\tau}_j / \hat{\tau}_{j'}$ . A first-order Taylor expansion around the true values gives:

$$\hat{\psi}_1 - \psi_1 = \nabla g(\tau_{k^*}, \tau_j, \tau_{j'})^\top \begin{pmatrix} \hat{\tau}_{k^*} - \tau_{k^*} \\ \hat{\tau}_j - \tau_j \\ \hat{\tau}_{j'} - \tau_{j'} \end{pmatrix} + o_p(n^{-1/2}) \quad (19)$$

$$= \frac{\tau_j}{\tau_{j'}} (\hat{\tau}_{k^*} - \tau_{k^*}) + \frac{\tau_{k^*}}{\tau_{j'}} (\hat{\tau}_j - \tau_j) - \frac{\tau_{k^*} \tau_j}{\tau_{j'}^2} (\hat{\tau}_{j'} - \tau_{j'}) + o_p(n^{-1/2}) \quad (20)$$

$$= R_1 (\hat{\tau}_{k^*} - \tau_{k^*}) + \frac{\psi_1}{\tau_j} (\hat{\tau}_j - \tau_j) - \frac{\psi_1}{\tau_{j'}} (\hat{\tau}_{j'} - \tau_{j'}) + o_p(n^{-1/2}). \quad (21)$$

Substituting the results:

$$\hat{\psi}_1 - \psi_1 = R_1 \cdot \mathbb{P}_n[\phi_{\tau_{k^*}}(O)] + \frac{\psi_1}{\tau_j} \cdot \mathbb{P}_n[\phi_{\tau_j}(O)] - \frac{\psi_1}{\tau_{j'}} \cdot \mathbb{P}_n[\phi_{\tau_{j'}}(O)] + o_p(n^{-1/2}) \quad (22)$$

$$= \mathbb{P}_n \left[ R_1 \cdot \phi_{\tau_{k^*}}(O) + \frac{\psi_1}{\tau_j} \phi_{\tau_j}(O) - \frac{\psi_1}{\tau_{j'}} \phi_{\tau_{j'}}(O) \right] + o_p(n^{-1/2}) \quad (23)$$

$$= \mathbb{P}_n[\phi_{\psi_1}(O)] + o_p(n^{-1/2}). \quad (24)$$

This establishes that  $\hat{\psi}_1$  is asymptotically linear with influence function  $\phi_{\psi_1}(O)$ —precisely the efficient influence function derived in Proposition 1. By the convolution theorem, any regular estimator has asymptotic variance at least  $\mathbb{E}[\phi_{\psi_1}(O)^2]$ , and  $\hat{\psi}_1$  achieves this bound.

**Strategy 2.** The same argument applies to  $\hat{\psi}_2 = \hat{\tau}_{k^*} \cdot \hat{\mu}_{c^*,\ell} / \hat{\mu}_{c^*,\ell'}$ . The Taylor expansion yields:

$$\hat{\psi}_2 - \psi_2 = R_2(\hat{\tau}_{k^*} - \tau_{k^*}) + \frac{\psi_2}{\bar{\mu}_{c^*,\ell}} (\hat{\mu}_{c^*,\ell} - \bar{\mu}_{c^*,\ell}) - \frac{\psi_2}{\bar{\mu}_{c^*,\ell'}} (\hat{\mu}_{c^*,\ell'} - \bar{\mu}_{c^*,\ell'}) + o_p(n^{-1/2}), \quad (25)$$

and substituting asymptotic linear representations gives  $\hat{\psi}_2 - \psi_2 = \mathbb{P}_n[\phi_{\psi_2}(O)] + o_p(n^{-1/2})$ .

**Remark 1.** *The plug-in estimator achieves efficiency because: (i) each building block is estimated using its own efficient influence function via doubly robust scores; (ii) the TATE is a smooth function of these building blocks; and (iii) the delta method preserves asymptotic linearity. This would fail if we used inefficient estimators for the building blocks (e.g., simple sample means without covariate adjustment) or if the function  $g$  were non-smooth at the true parameter values.*

#### B.4 Proof of Theorem 4

*Proof of Part (a): Asymptotic Normality.* We prove the result for  $\hat{\psi}_1$ ; the proofs for  $\hat{\psi}_2$  and  $\hat{\psi}_2^*$  follow analogously.

*Step 1: Asymptotic linearity of building blocks.* By Lemma 1, the score  $\varphi_{\tau_k}(O; \eta)$  satisfies Neyman orthogonality. Combined with Assumption 6, standard arguments from Chernozhukov et al. [2018] establish that:

$$\hat{\tau}_k - \tau_k = \mathbb{P}_n[\phi_{\tau_k}(O)] + o_p(n^{-1/2}) \quad \text{for } k \in \{k^*, j, j'\}.$$

To see this, write:

$$\begin{aligned} \hat{\tau}_k - \tau_k &= \mathbb{P}_n[\varphi_{\tau_k}(O; \hat{\eta})] - \tau_k \\ &= \mathbb{P}_n[\varphi_{\tau_k}(O; \hat{\eta}) - \varphi_{\tau_k}(O; \eta)] + \mathbb{P}_n[\varphi_{\tau_k}(O; \eta)] - \tau_k + \tau_k - \tau_k \\ &= \mathbb{P}_n[\phi_{\tau_k}(O)] + \mathbb{P}_n[\varphi_{\tau_k}(O; \hat{\eta}) - \varphi_{\tau_k}(O; \eta)]. \end{aligned}$$

The second term is  $o_p(n^{-1/2})$  by Neyman orthogonality and Assumption 6. Specifically, a second-order expansion around the true  $\eta$  shows:

$$\begin{aligned} \mathbb{P}_n[\varphi_{\tau_k}(O; \hat{\eta}) - \varphi_{\tau_k}(O; \eta)] &= O_p(\|\hat{\eta} - \eta\|_2^2) + O_p(\|\hat{\mu}_{a,k} - \mu_{a,k}\|_2 \cdot \|\hat{\pi}_k - \pi_k\|_2) \\ &\quad + O_p(\|\hat{\mu}_{a,k} - \mu_{a,k}\|_2 \cdot \|\hat{e}_k - e_k\|_2), \end{aligned}$$

which is  $o_p(n^{-1/2})$  under Assumption 6.

*Step 2: Delta method.* Define  $\boldsymbol{\tau} = (\tau_{k^*}, \tau_j, \tau_{j'})^\top$  and  $\hat{\boldsymbol{\tau}} = (\hat{\tau}_{k^*}, \hat{\tau}_j, \hat{\tau}_{j'})^\top$ . The function  $g(x, y, z) = xy/z$  is continuously differentiable in a neighborhood of  $\boldsymbol{\tau}$  by Assumption 5(iii), which ensures  $\tau_{j'} \neq 0$ .

By the functional delta method [van der Vaart, 1998]:

$$\begin{aligned} \hat{\psi}_1 - \psi_1 &= g(\hat{\boldsymbol{\tau}}) - g(\boldsymbol{\tau}) \\ &= \nabla g(\boldsymbol{\tau})^\top (\hat{\boldsymbol{\tau}} - \boldsymbol{\tau}) + o_p(\|\hat{\boldsymbol{\tau}} - \boldsymbol{\tau}\|) \\ &= \nabla g(\boldsymbol{\tau})^\top \mathbb{P}_n[\boldsymbol{\phi}_{\boldsymbol{\tau}}(O)] + o_p(n^{-1/2}) \\ &= \mathbb{P}_n[\phi_{\psi_1}(O)] + o_p(n^{-1/2}), \end{aligned}$$

where  $\boldsymbol{\phi}_{\boldsymbol{\tau}}(O) = (\phi_{\tau_{k^*}}(O), \phi_{\tau_j}(O), \phi_{\tau_{j'}}(O))^\top$  and  $\phi_{\psi_1}(O) = \nabla g(\boldsymbol{\tau})^\top \boldsymbol{\phi}_{\boldsymbol{\tau}}(O)$  as derived in Proposition 2.

*Step 3: Central limit theorem.* By Lemma 1,  $\mathbb{E}[\phi_{\tau_k}(O)] = 0$  for each  $k$ , which implies  $\mathbb{E}[\phi_{\psi_1}(O)] = 0$ . The variance  $V_1 := \mathbb{E}[\phi_{\psi_1}(O)^2]$  is finite by Lemma 1(iii) and the continuous mapping theorem.

The Lindeberg-Lévy central limit theorem yields:

$$\sqrt{n} \mathbb{P}_n[\phi_{\psi_1}(O)] \xrightarrow{d} \mathcal{N}(0, V_1).$$

Combined with Step 2:

$$\sqrt{n}(\hat{\psi}_1 - \psi_1) = \sqrt{n} \mathbb{P}_n[\phi_{\psi_1}(O)] + o_p(1) \xrightarrow{d} \mathcal{N}(0, V_1).$$

Step 4: Variance estimation. By the continuous mapping theorem and consistency of  $\hat{\eta}$ :

$$\hat{V}_1 = \mathbb{P}_n[\hat{\phi}_{\psi_1}^2] \xrightarrow{p} \mathbb{E}[\phi_{\psi_1}(O)^2] = V_1.$$

Extension to  $\hat{\psi}_2$  and  $\hat{\psi}_2^*$ . The proof for  $\hat{\psi}_2$  is identical, replacing  $(\tau_j, \tau_{j'})$  with  $(\bar{\mu}_{c^*, \ell}, \bar{\mu}_{c^*, \ell'})$ . For  $\hat{\psi}_2^*$ , the estimated weights  $\hat{\mathbf{w}}^*$  introduce additional terms that are  $o_p(n^{-1/2})$  by Assumption 6 and Slutsky's theorem.  $\square$

*Proof of Part (b): Double Robustness.* It suffices to show that  $\mathbb{E}[\varphi_{a,k}(O; \hat{\eta})] = \bar{\mu}_{a,k}$  when either condition (a) or (b) holds, since the TATE estimators are continuous functions of marginal means.

*Case (a): Outcome model correctly specified.* Suppose  $\mu_{a,k}(X) = \mathbb{E}[Y \mid A = a, S = k, X]$  but propensity scores may be misspecified as  $\tilde{\pi}_k(X)$  and  $\tilde{e}_k(a, X)$ . Write:

$$\mathbb{E}[\varphi_{a,k}(O; \hat{\eta})] = \mathbb{E}\left[\frac{\mathbf{1}[S = k]}{\tilde{\pi}_k(X)} \cdot \frac{\mathbf{1}[A = a]}{\tilde{e}_k(a, X)} (Y - \mu_{a,k}(X))\right] + \mathbb{E}\left[\frac{\mathbf{1}[S = k]}{\tilde{\pi}_k(X)} \mu_{a,k}(X)\right].$$

The first term equals zero since  $\mathbb{E}[Y - \mu_{a,k}(X) \mid A = a, S = k, X] = 0$  by correct specification of the outcome model, regardless of the propensity score specification.

Under random sampling (Assumption 2(i) or 4(i)),  $\pi_k(X) = p_k := P(S = k)$  is constant. Thus  $\tilde{\pi}_k(X) = p_k$  is correctly specified as the empirical proportion  $n_k/n$ , and the second term equals:

$$\mathbb{E}\left[\frac{\mathbf{1}[S = k]}{p_k} \mu_{a,k}(X)\right] = \frac{P(S = k)}{p_k} \mathbb{E}[\mu_{a,k}(X) \mid S = k] = \mathbb{E}[\mu_{a,k}(X) \mid S = k] = \bar{\mu}_{a,k}.$$

*Case (b): Both propensity scores correctly specified.* Suppose  $\pi_k(X) = P(S = k \mid X)$  and  $e_k(a, X) = P(A = a \mid S = k, X)$  are correct, but  $\tilde{\mu}_{a,k}(X)$  may be misspecified. Then:

$$\mathbb{E}[\varphi_{a,k}(O; \hat{\eta})] = \mathbb{E}\left[\frac{\mathbf{1}[S = k]}{\pi_k(X)} \cdot \frac{\mathbf{1}[A = a]}{e_k(a, X)} Y\right] - \mathbb{E}\left[\frac{\mathbf{1}[S = k]}{\pi_k(X)} \left(\frac{\mathbf{1}[A = a]}{e_k(a, X)} - 1\right) \tilde{\mu}_{a,k}(X)\right].$$

For the first term, conditioning on  $(S, X)$ :

$$\begin{aligned} \mathbb{E}\left[\frac{\mathbf{1}[S = k]}{\pi_k(X)} \cdot \frac{\mathbf{1}[A = a]}{e_k(a, X)} Y\right] &= \mathbb{E}\left[\frac{\mathbf{1}[S = k]}{\pi_k(X)} \cdot \frac{e_k(a, X)}{e_k(a, X)} \mathbb{E}[Y \mid A = a, S = k, X]\right] \\ &= \mathbb{E}\left[\frac{\mathbf{1}[S = k]}{\pi_k(X)} \mu_{a,k}(X)\right] \\ &= \bar{\mu}_{a,k}. \end{aligned}$$

For the second term:

$$\mathbb{E}\left[\frac{\mathbf{1}[A = a]}{e_k(a, X)} - 1 \mid S = k, X\right] = \frac{P(A = a \mid S = k, X)}{e_k(a, X)} - 1 = 0,$$

so the second term vanishes by the law of iterated expectations.  $\square$

*Proof of Part (c): Efficiency of Combined Estimator. Step 1: Optimal weights for ratio combination.* Consider estimators of the form  $\hat{R} = \mathbf{w}^\top \hat{\mathbf{R}}$  where  $\mathbf{w}^\top \mathbf{1} = 1$ . Under the null that all  $R_{2,j}$  equal a common value  $R_2$ , the asymptotic variance of  $\sqrt{n}(\hat{R} - R_2)$  is:

$$V_R(\mathbf{w}) = \mathbf{w}^\top \mathbf{V}_R \mathbf{w}.$$

To minimize  $V_R(\mathbf{w})$  subject to  $\mathbf{w}^\top \mathbf{1} = 1$ , form the Lagrangian:

$$\mathcal{L}(\mathbf{w}, \lambda) = \mathbf{w}^\top \mathbf{V}_R \mathbf{w} - \lambda(\mathbf{w}^\top \mathbf{1} - 1).$$

First-order conditions:

$$\frac{\partial \mathcal{L}}{\partial \mathbf{w}} = 2\mathbf{V}_R \mathbf{w} - \lambda \mathbf{1} = 0 \quad \Rightarrow \quad \mathbf{w} = \frac{\lambda}{2} \mathbf{V}_R^{-1} \mathbf{1}.$$

Applying the constraint  $\mathbf{w}^\top \mathbf{1} = 1$ :

$$\frac{\lambda}{2} \mathbf{1}^\top \mathbf{V}_R^{-1} \mathbf{1} = 1 \quad \Rightarrow \quad \frac{\lambda}{2} = \frac{1}{\mathbf{1}^\top \mathbf{V}_R^{-1} \mathbf{1}}.$$

Thus:

$$\mathbf{w}^* = \frac{\mathbf{V}_R^{-1} \mathbf{1}}{\mathbf{1}^\top \mathbf{V}_R^{-1} \mathbf{1}}.$$

The minimized variance is:

$$V_{R_2^*} = \mathbf{w}^{*\top} \mathbf{V}_R \mathbf{w}^* = \frac{\mathbf{1}^\top \mathbf{V}_R^{-1} \mathbf{V}_R \mathbf{V}_R^{-1} \mathbf{1}}{(\mathbf{1}^\top \mathbf{V}_R^{-1} \mathbf{1})^2} = \frac{1}{\mathbf{1}^\top \mathbf{V}_R^{-1} \mathbf{1}}.$$

*Step 2: Variance of combined TATE estimator.* When the target trial  $k^*$  is distinct from all anchor trials, the influence functions  $\phi_{\tau_{k^*}}(O)$  and  $\phi_{R_{2,j}}(O)$  have disjoint support (they involve indicators for different trials). Thus:

$$\mathbb{E}[\phi_{\tau_{k^*}}(O) \cdot \phi_{R_{2,j}}(O)] = 0 \quad \text{for all } j.$$

The variance of  $\psi_2^* = \tau_{k^*} \cdot R_2^*$  is therefore:

$$\begin{aligned} V_{\psi_2^*} &= \mathbb{E}[\phi_{\psi_2^*}(O)^2] = \mathbb{E} \left[ \left( R_2^* \cdot \phi_{\tau_{k^*}}(O) + \tau_{k^*} \sum_{j=1}^m w_j^* \phi_{R_{2,j}}(O) \right)^2 \right] \\ &= R_2^{*2} \mathbb{E}[\phi_{\tau_{k^*}}(O)^2] + \tau_{k^*}^2 \mathbb{E} \left[ \left( \sum_{j=1}^m w_j^* \phi_{R_{2,j}}(O) \right)^2 \right] \\ &= R_2^{*2} V_{\tau_{k^*}} + \tau_{k^*}^2 V_{R_2^*}. \end{aligned}$$

Since  $\mathbf{w}^*$  minimizes  $V_{R_2^*}$ , the estimator  $\hat{\psi}_2^* = \hat{\tau}_{k^*} \cdot \hat{R}_2^*$  achieves minimum asymptotic variance among estimators of the specified form.  $\square$

## B.5 Specification Test Derivation

**Specification test.** Under Assumption 3, all ratios equal a common value:  $R_{2,1} = \dots = R_{2,m}$ . This provides  $m - 1$  testable restrictions. Let  $\mathbf{C} \in \mathbb{R}^{(m-1) \times m}$  be a contrast matrix (e.g.,  $C_{j,j} = 1$ ,  $C_{j,j+1} = -1$  for successive differences). Under  $H_0$ :

$$Q = n \cdot (\mathbf{C}\hat{\mathbf{R}})^\top (\mathbf{C}\hat{\mathbf{V}}_R \mathbf{C}^\top)^{-1} (\mathbf{C}\hat{\mathbf{R}}) \xrightarrow{d} \chi_{m-1}^2. \quad (26)$$

Rejection indicates that different anchors yield systematically different ratios, suggesting  $\Lambda$  depends on intervention timing. This would occur, for instance, if treatment effects decay over time since administration—a violation of Assumption 3 that Strategy 1 can accommodate. Note that failure to reject does not validate Assumption 3; the test has power only against alternatives where different arms exhibit detectably different temporal scaling.

**Proposition 6** (Asymptotic Distribution of Specification Test). *Under  $H_0 : R_{2,1} = \dots = R_{2,m}$  and Assumptions 5–6, the test statistic  $Q$  defined in (26) satisfies  $Q \xrightarrow{d} \chi_{m-1}^2$ .*

*Proof.* Under  $H_0$ , all ratios  $R_{2,j}$  equal a common value  $R_2$ , so  $\mathbf{C}\mathbf{R} = \mathbf{0}$  where  $\mathbf{C} \in \mathbb{R}^{(m-1) \times m}$  is the contrast matrix.

By Theorem 4(a),  $\sqrt{n}(\hat{\mathbf{R}} - \mathbf{R}) \xrightarrow{d} \mathcal{N}(\mathbf{0}, \mathbf{V}_R)$ . By the continuous mapping theorem:

$$\sqrt{n} \mathbf{C}\hat{\mathbf{R}} = \sqrt{n} \mathbf{C}(\hat{\mathbf{R}} - \mathbf{R}) \xrightarrow{d} \mathcal{N}(\mathbf{0}, \mathbf{C}\mathbf{V}_R \mathbf{C}^\top).$$

The matrix  $\mathbf{C}\mathbf{V}_R\mathbf{C}^\top \in \mathbb{R}^{(m-1) \times (m-1)}$  is positive definite since  $\mathbf{V}_R$  is positive definite and  $\mathbf{C}$  has full row rank. Therefore:

$$Q = n \cdot (\mathbf{C}\hat{\mathbf{R}})^\top (\mathbf{C}\mathbf{V}_R\mathbf{C}^\top)^{-1} (\mathbf{C}\hat{\mathbf{R}}) \xrightarrow{d} \chi_{m-1}^2.$$

By Slutsky's theorem and consistency of  $\hat{\mathbf{V}}_R$ , replacing  $\mathbf{V}_R$  with  $\hat{\mathbf{V}}_R$  does not affect the limiting distribution.  $\square$

## B.6 TMLE-Style Estimation

Targeted Minimum Loss-based Estimation (TMLE) provides an alternative construction that directly solves the efficient influence function estimating equation. We describe two approaches: a factorized TMLE that targets each building block separately, and a joint TMLE that targets the TATE directly.

### B.6.1 Factorized TMLE

The factorized approach applies TMLE separately to each building block, then combines via plug-in.

**Step 1: Initial estimates.** Obtain initial estimates  $\hat{\mu}_{a,k}^{(0)}(X)$  of the outcome regressions using any consistent method (e.g., random forests, gradient boosting).

**Step 2: Targeting each conditional mean.** For each  $(a, k)$  pair, we fluctuate the initial estimate to solve  $\mathbb{P}_n[\phi_{\hat{\mu}_{a,k}}(O; \eta^*)] = 0$ . Define the clever covariate:

$$H_{a,k}(S, A, X) = \frac{\mathbf{1}[S = k]}{\pi_k(X)} \cdot \frac{\mathbf{1}[A = a]}{e_k(a, X)}. \quad (27)$$

For continuous outcomes, fit a linear fluctuation:

$$\hat{\mu}_{a,k}^*(X) = \hat{\mu}_{a,k}^{(0)}(X) + \hat{\epsilon}_{a,k}, \quad (28)$$

where  $\hat{\epsilon}_{a,k}$  solves:

$$\sum_{i=1}^n H_{a,k}(S_i, A_i, X_i) \cdot (Y_i - \hat{\mu}_{a,k}^{(0)}(X_i) - \epsilon_{a,k}) = 0. \quad (29)$$

This has closed-form solution:

$$\hat{\epsilon}_{a,k} = \frac{\sum_{i=1}^n H_{a,k}(S_i, A_i, X_i) \cdot (Y_i - \hat{\mu}_{a,k}^{(0)}(X_i))}{\sum_{i=1}^n H_{a,k}(S_i, A_i, X_i)}. \quad (30)$$

For binary/bounded outcomes, use a logistic fluctuation to respect the outcome space:

$$\text{logit}(\hat{\mu}_{a,k}^*(X)) = \text{logit}(\hat{\mu}_{a,k}^{(0)}(X)) + \hat{\epsilon}_{a,k} \cdot H_{a,k}(S, A, X), \quad (31)$$

where  $\hat{\epsilon}_{a,k}$  is obtained by logistic regression of  $Y$  on  $H_{a,k}$  with offset  $\text{logit}(\hat{\mu}_{a,k}^{(0)}(X))$ .

**Step 3: Construct targeted building blocks.** The targeted estimates of marginal means and ATEs are:

$$\hat{\mu}_{a,k}^* = \mathbb{P}_n \left[ \frac{\mathbf{1}[S = k]}{\pi_k(X)} \cdot \hat{\mu}_{a,k}^*(X) \right], \quad (32)$$

$$\hat{\tau}_k^* = \hat{\mu}_{a_k,k}^* - \hat{\mu}_{b_k,k}^*. \quad (33)$$

**Step 4: Plug-in for TATE.** The factorized TMLE estimators are:

$$\hat{\psi}_1^{\text{TMLE}} = \hat{\tau}_{k^*}^* \cdot \frac{\hat{\tau}_j^*}{\hat{\tau}_{j'}^*}, \quad (34)$$

$$\hat{\psi}_2^{\text{TMLE}} = \hat{\tau}_{k^*}^* \cdot \frac{\hat{\mu}_{c^*,\ell}^*}{\hat{\mu}_{c^*,\ell'}^*}. \quad (35)$$

By construction, each building block solves its own EIF equation:  $\mathbb{P}_n[\phi_{\hat{\mu}_{a,k}}(O; \hat{\eta}^*)] = 0$ . Under standard regularity conditions, the factorized TMLE achieves the same asymptotic efficiency as the plug-in estimator.

## B.6.2 Joint TMLE

A more ambitious approach directly targets the TATE by jointly fluctuating all outcome models to solve  $\mathbb{P}_n[\phi_\psi(O; \eta^*)] = 0$ .

**Clever covariates for  $\psi_1$ .** The EIF for Strategy 1 is:

$$\phi_{\psi_1}(O) = R_1 \cdot \phi_{\tau_{k^*}}(O) + \frac{\psi_1}{\tau_j} \phi_{\tau_j}(O) - \frac{\psi_1}{\tau_{j'}} \phi_{\tau_{j'}}(O). \quad (36)$$

Expanding  $\phi_{\tau_k}(O)$  in terms of the outcome models and collecting terms, the clever covariate for  $\mu_{a,k}(X)$  is:

$$H_{a,k}^{\psi_1}(O) = \frac{\mathbf{1}[S = k]}{\pi_k(X)} \cdot \frac{\mathbf{1}[A = a]}{e_k(a, X)} \cdot \omega_{a,k}, \quad (37)$$

where the weights  $\omega_{a,k}$  depend on which trial and arm:

$$\omega_{a,k} = \begin{cases} +R_1 & \text{if } k = k^*, a = a_{k^*} \\ -R_1 & \text{if } k = k^*, a = b_{k^*} \\ +\psi_1/\tau_j & \text{if } k = j, a = a_j \\ -\psi_1/\tau_j & \text{if } k = j, a = b_j \\ -\psi_1/\tau_{j'} & \text{if } k = j', a = a_{j'} \\ +\psi_1/\tau_{j'} & \text{if } k = j', a = b_{j'} \\ 0 & \text{otherwise} \end{cases} \quad (38)$$

**Iterative targeting algorithm.** Since the weights  $\omega_{a,k}$  depend on unknown parameters  $(R_1, \psi_1, \tau_j, \tau_{j'})$ , joint TMLE requires iteration:

1. **Initialize:** Obtain initial estimates  $\hat{\mu}_{a,k}^{(0)}(X)$  and compute initial  $\hat{\tau}_{k^*}^{(0)}, \hat{\tau}_j^{(0)}, \hat{\tau}_{j'}^{(0)}, \hat{R}_1^{(0)}, \hat{\psi}_1^{(0)}$ .
2. **Compute weights:** Using current parameter estimates, compute  $\hat{\omega}_{a,k}^{(t)}$ .
3. **Single joint fluctuation:** Fit a single  $\epsilon$  across all outcome models:

$$\hat{\epsilon}^{(t)} = \arg \min_{\epsilon} \sum_{i=1}^n \sum_{(a,k)} L(Y_i, \hat{\mu}_{a,k}^{(t)}(X_i) + \epsilon \cdot H_{a,k}^{\psi_1}(O_i; \hat{\omega}_{a,k}^{(t)})), \quad (39)$$

where  $L$  is an appropriate loss (squared error for continuous, log-loss for binary).

4. **Update:** Set  $\hat{\mu}_{a,k}^{(t+1)}(X) = \hat{\mu}_{a,k}^{(t)}(X) + \hat{\epsilon}^{(t)} \cdot \hat{\omega}_{a,k}^{(t)}$  and recompute parameters.
5. **Iterate:** Repeat steps 2–4 until  $|\hat{\epsilon}^{(t)}| < \delta$  for some tolerance  $\delta$ .

Upon convergence, the joint TMLE solves  $\mathbb{P}_n[\phi_{\psi_1}(O; \hat{\eta}^*)] \approx 0$  up to the convergence tolerance.

## B.6.3 Comparison of Approaches

Property	Plug-in / Factorized TMLE	Joint TMLE
Solves $\mathbb{P}_n[\phi_\psi] = 0$	Asymptotically	Exactly (up to tolerance)
Asymptotic efficiency	Yes	Yes
Finite-sample bias	Second-order	Potentially smaller
Implementation	Simple	Iterative, complex
Numerical stability	High	May have convergence issues

**When does joint TMLE help?** The plug-in and factorized TMLE estimators are asymptotically equivalent to joint TMLE—all achieve the semiparametric efficiency bound. Joint TMLE may offer advantages when:

- Sample sizes are small, where exactly solving the EIF equation can reduce finite-sample bias
- Building blocks have near-zero denominators ( $\tau_{j'} \approx 0$  or  $\bar{\mu}_{c^*, \ell'} \approx 0$ ), where numerical stability from direct targeting may help
- One desires inference based on the EIF equation residual (e.g., for diagnostics)

In most settings with moderate sample sizes, the simpler plug-in approach performs comparably. We therefore recommend the plug-in estimator as the default, with joint TMLE as a robustness check when building block estimates are noisy or near boundary cases.

## C Upworthy Case Study

This appendix provides complete details for the empirical application in Section 7.

### C.1 Data Description

The Upworthy Research Archive [Matias et al., 2021] contains results from over 22,000 headline A/B tests conducted by Upworthy, a viral content website, from early 2013 through April 2015.<sup>5</sup> The archive includes 105,551 unique headline-image “packages” tested across these experiments.

**Experimental design.** For each article, Upworthy editors created multiple headline-image combinations. Website visitors were randomly assigned to view one package, with each test comparing between 2 and 24 alternatives. The archive provides aggregate results: impressions (number of visitors assigned to each package) and clicks (number who clicked through to the article). The primary outcome is click-through rate (CTR).

**Data cleaning.** Following guidance from the archive creators, we exclude tests conducted between June 2013 and January 2014, a period during which randomization problems were detected [Matias et al., 2021]. Our analysis focuses on tests from February 2014 onward.

### C.2 Identifying Treatment Arms Across Tests

A key challenge in applying our framework is identifying treatment arms that appear across multiple tests at different times. Each A/B test uses unique headline text, so we cannot directly match treatments across tests. Instead, we cluster semantically similar headlines into groups that can be tracked across experiments.

**Constrained clustering problem.** We frame this as a constrained clustering problem with a key restriction: within each test, every headline represents a *distinct* treatment arm, so no two headlines from the same test should be assigned to the same cluster. Standard clustering algorithms do not enforce such constraints.

**Three-step procedure.** Our approach proceeds as follows:

1. **Embedding.** We embed each headline using Sentence-BERT [Reimers and Gurevych, 2019], specifically the all-MiniLM-L6-v2 model, which maps sentences to 384-dimensional dense vectors optimized for semantic similarity.
2. **Centroid initialization.** We perform  $K$ -means clustering on the full set of headline embeddings to obtain  $K = 50$  cluster centroids. This provides a set of representative “headline styles” in the embedding space.
3. **Constrained assignment.** For each test, we solve a minimum-cost bipartite matching problem using the Hungarian algorithm [Kuhn, 1955]. The cost matrix contains Euclidean distances between each headline’s embedding and each cluster centroid. The matching assigns each headline to a unique cluster while minimizing total distance, ensuring that headlines within the same test receive different cluster labels.

---

<sup>5</sup>Available at <https://osf.io/jd64p/>.

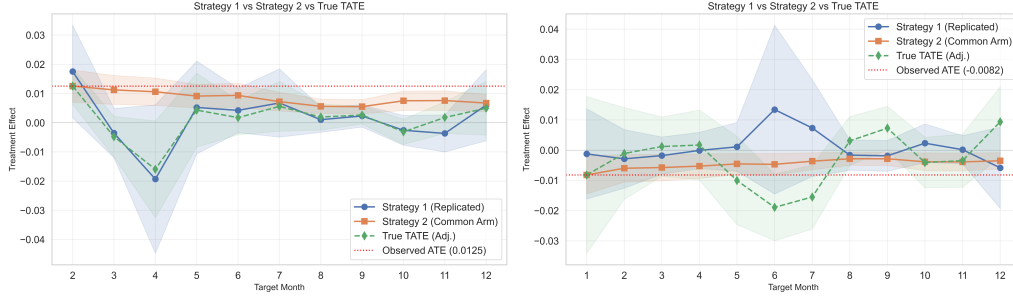


Figure 3: TATE estimates by target month for both trials. Each panel shows Strategy 1 (Replicated Trials; blue circles), Strategy 2 (Common Arm; orange squares), and true TATE (green diamonds) with 95% confidence bands. Dashed red line indicates observed ATE at source time. Left: Trial A (Cluster 17 vs. 10), source time January 2014. Right: Trial B (Cluster 46 vs. 12), source time December 2013.

**Cluster characteristics.** The resulting 50 clusters range in size from 1,792 to 11,626 headlines (mean: 5,278). Manual inspection confirms semantically coherent groupings. Crucially, all clusters appear in tests conducted across multiple quarters of our study period, providing the temporal variation necessary for identifying temporal ratios.

### C.3 Experimental Setup

**Trial selection.** We select two trials with sufficient data for both identification strategies:

- **Trial A** (test ID: 52f54b9ab17b): Compares Cluster 17 against Cluster 10, conducted in January 2014. Observed ATE: +0.0125 (Cluster 17 headlines achieved 1.25 percentage points higher CTR).
- **Trial B** (test ID: 52e1c6cca01f): Compares Cluster 46 against Cluster 12, conducted in December 2013. Observed ATE:  $-0.0082$  (Cluster 46 headlines achieved 0.82 percentage points lower CTR).

**Strategy implementation.** For Strategy 1 (Replicated Trials), we identify all tests comparing the same cluster pair as the target trial and estimate temporal ratios from ATE ratios across time periods. For Strategy 2 (Common Arm), we select the 10 anchor arms with the highest observation counts at both source and target measurement times. We estimate temporal ratios from each anchor arm separately, then combine them using inverse-variance weighting as described in Section 4.

**Ground truth construction.** To evaluate estimator performance, we construct a “true” TATE at each target month by pooling all available comparisons of the same cluster pair during that month. We normalize so that the true TATE equals the observed ATE at the source time, enabling direct comparison of temporal dynamics.

### C.4 Complete Results

Figure 3 displays TATE estimates for both trials across all target months of 2014.

**Variance-bias tradeoff.** The results reveal a clear variance-bias tradeoff between strategies. Strategy 2 yields substantially smaller standard errors than Strategy 1: for Trial A, mean standard errors are 0.0019 versus 0.0054; for Trial B, 0.0018 versus 0.0053. This precision advantage reflects Strategy 2’s use of conditional means rather than treatment effect contrasts to estimate temporal ratios.

However, Strategy 2 exhibits systematic bias. In Trial A (Figure 3, left panel), Strategy 2 estimates remain uniformly positive throughout the year, while the true TATE varies considerably—turning negative in March, April, and October. Strategy 1, despite wider confidence bands, tracks these sign changes. Trial B shows a similar pattern: Strategy 2 remains negative throughout while the true TATE is positive in several months.

**Tracking temporal dynamics.** Strategy 1 estimates exhibit higher volatility but move directionally with the true TATE. The correlation between Strategy 1 and true TATE is 0.71 for Trial A and 0.52 for Trial B, compared to 0.35 and 0.18 for Strategy 2. Strategy 2’s smoother trajectory reflects pooling across multiple anchor arms, which reduces noise but dampens responsiveness to treatment-specific temporal dynamics.

**Aggregate accuracy.** Neither strategy uniformly dominates. Strategy 1 achieves lower RMSE in both trials (0.0062 vs. 0.0080 for Trial A; 0.0090 vs. 0.0101 for Trial B), as Strategy 2’s bias outweighs its precision advantage in this application.

## C.5 Interpretation and Limitations

**Why does Strategy 2 exhibit bias?** The systematic bias in Strategy 2 suggests violations of Assumption 3, which requires that the temporal modifier depend only on measurement time:  $\Lambda(t_0, t_1) = \Lambda(t_1)$ . This assumption fails when the temporal factor depends on both intervention time  $t_0$  and measurement time  $t_1$ —or equivalently, when the duration between intervention and measurement matters.

One scenario where this occurs is treatment effect decay: if the effect of an intervention diminishes as time passes since administration, then  $\Lambda(t_0, t_1)$  depends on the gap  $t_1 - t_0$ , not just  $t_1$ . This is plausible in the headline testing context. Exposure to a headline likely produces effects that decay over time—initial engagement may be high, but the influence on click behavior diminishes as users encounter other content or as the novelty fades. When such decay dynamics are present, Strategy 2’s restriction to  $\Lambda(t_1)$  introduces bias, while Strategy 1’s more flexible structure  $\Lambda(t_0, t_1)$  can accommodate the dependence on intervention timing.

When both strategies are feasible, comparing estimates provides a robustness check. Substantial discrepancies, as observed in Figure 3, signal potential violations of Assumption 3 and suggest preferring Strategy 1 despite its higher variance.

**Limitations.** Several caveats apply to this analysis:

- The “true” TATE is itself estimated from data and subject to sampling error, particularly in months with fewer observations.
- Semantic clustering introduces measurement error: headlines within a cluster are similar but not identical. This may attenuate estimated effects and introduce noise in temporal ratio estimates.
- The Upworthy platform evolved during the study period (design changes, audience growth), potentially confounding temporal variation in engagement with platform-level changes.
- Our analysis treats headline clusters as discrete treatments, but the clustering is necessarily a simplification of continuous variation in headline characteristics.